Hypernuclear Research at MAMI, GSI and FAIR

Patrick Achenbach

U Mainz

Sept. 2o12

Hot spots of hypernuclear physics

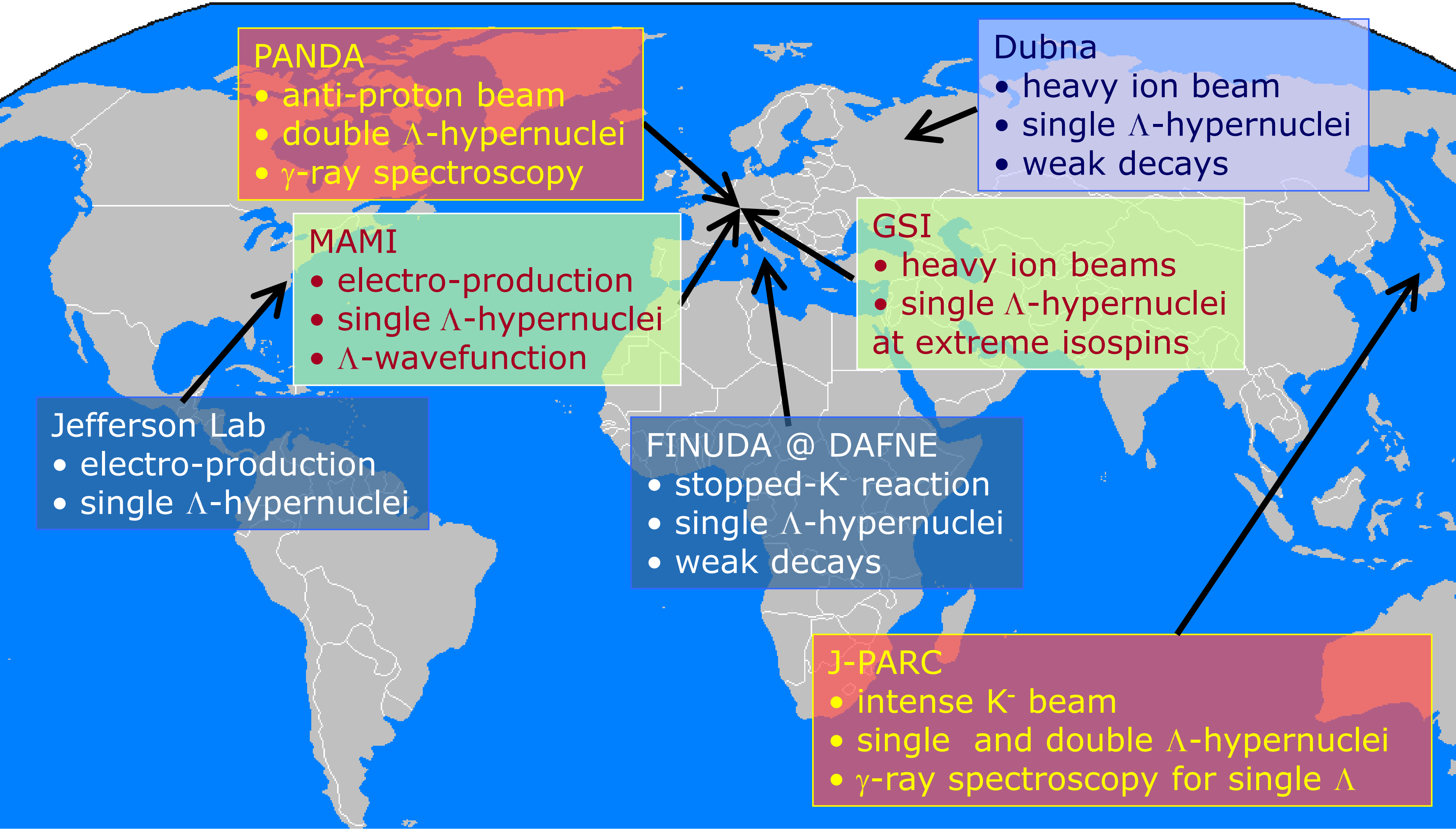

Hot spots of hypernuclear physics

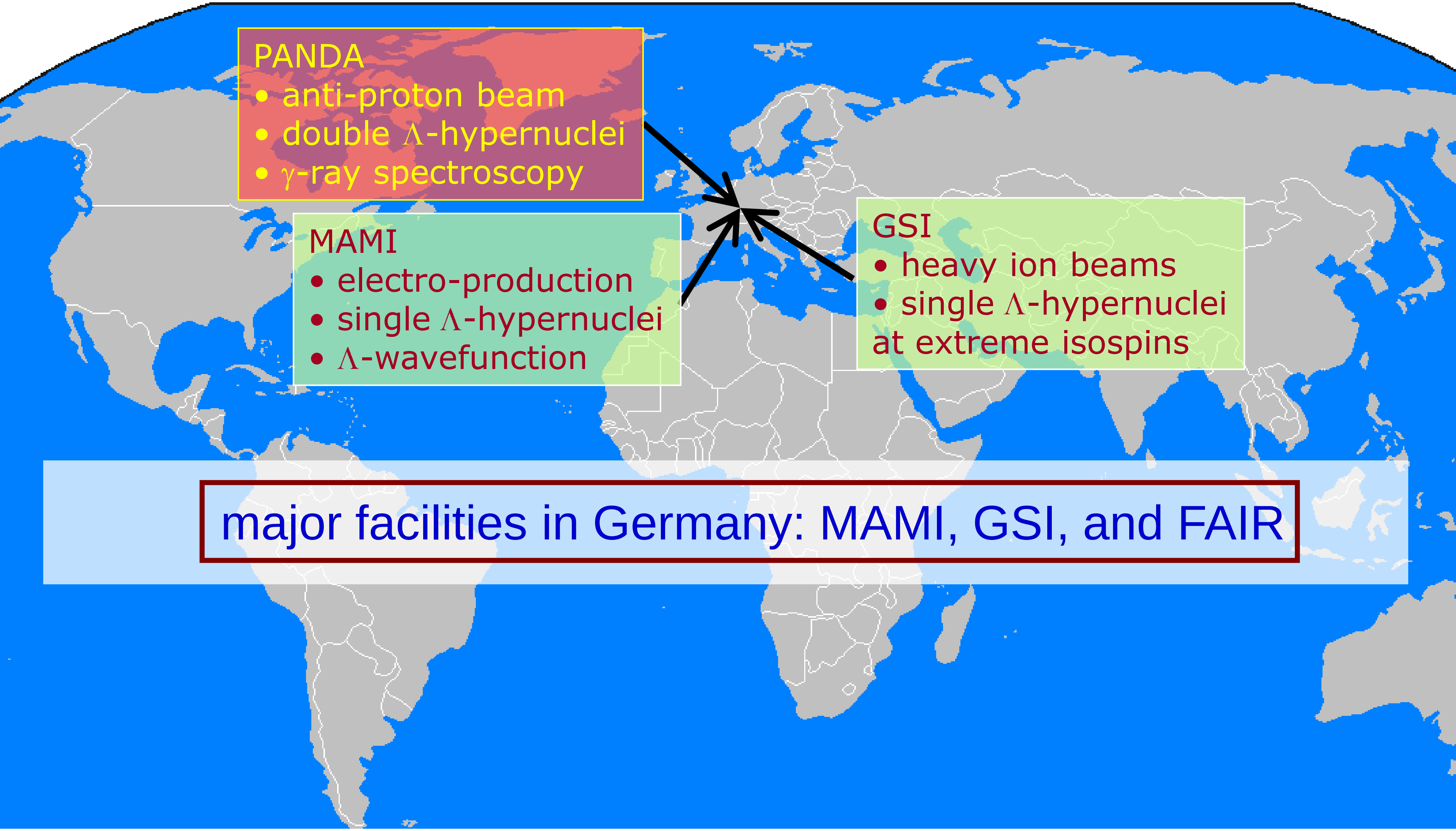

Hot spots of hypernuclear physics

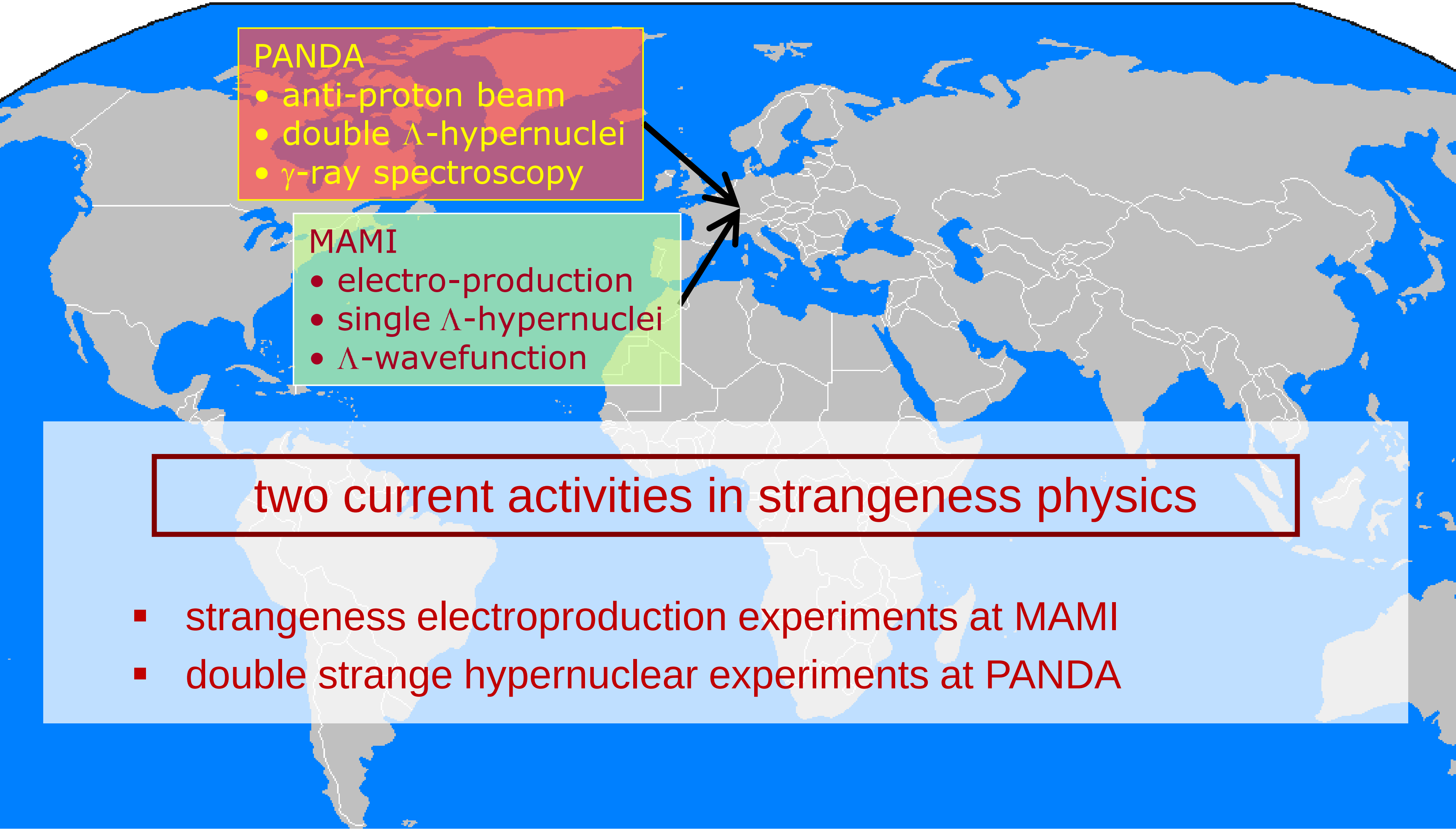

two current activities in strangeness physics

- strangeness electroproduction experiments at MAMI
- double strange hypernuclear experiments at PANDA

Electroproduction of hypernuclei and hyperfragments

Role of kaon electroproduction for strangeness formation

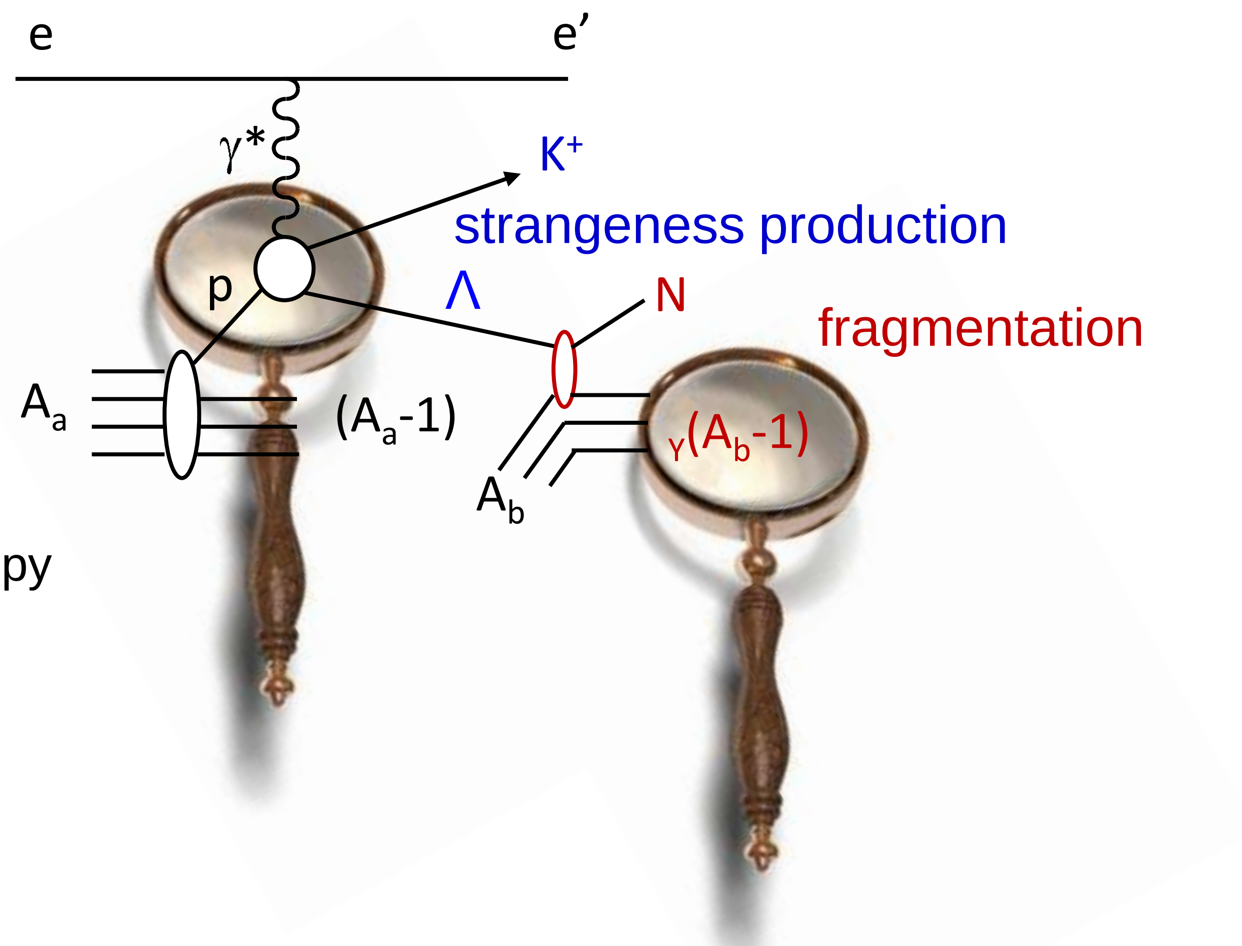

Formation mechanisms:
- strangeness exchange
- strangeness production
  - by strong interaction
  - electroproduction

Spectroscopic methods:
- missing mass spectroscopy
- gamma spectroscopy
- decay spectroscopy

Electroproduction of strangeness is providing a magnifying glass for ...
strangeness structure of proton excitations
and strange nuclear fragment production

$p(e,e'K)\Lambda$ in the one-photon-exchange approximation

five-fold differential cross section separates in **virtual photon flux** and **virtual photoproduction**

$$\frac{d\sigma}{dE'd\Omega_{e'}d\Omega_K^*} = \boxed{\Gamma}\boxed{\frac{d\sigma}{d\Omega_K^*}}$$

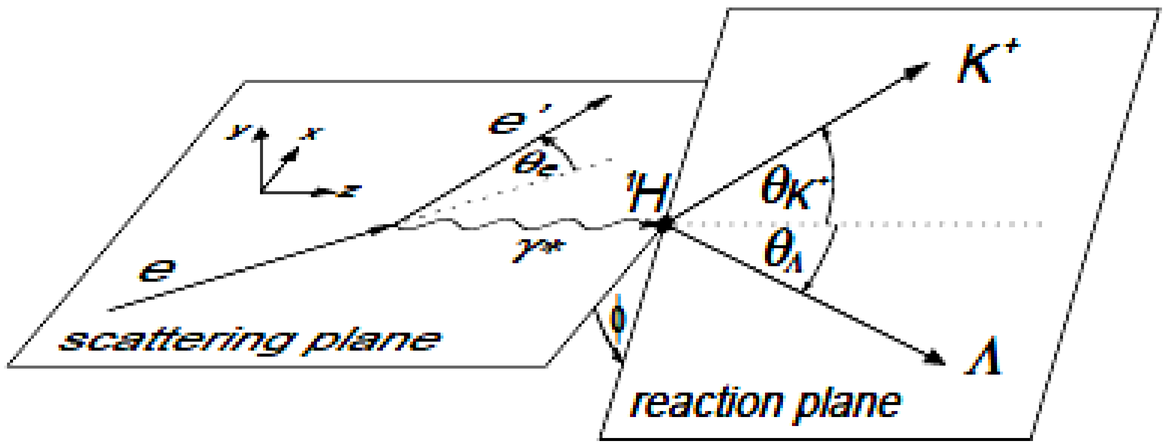

structure of **virtual photoproduction** cross section:

$$\frac{d\sigma}{d\Omega_K^*} = \sigma_T + \epsilon\sigma_L + \epsilon\sigma_{TT}\cos 2\phi + \sqrt{2\epsilon(1+\epsilon)}\sigma_{LT}\cos\phi + h\sqrt{2\epsilon(1-\epsilon)}\sigma_{LT'}\sin\phi$$

for polarized electrons with helicity *h*: $A_{LT'} = \frac{\frac{d\sigma}{d\Omega_K^*}^+ - \frac{d\sigma}{d\Omega_K^*}^-}{\frac{d\sigma}{d\Omega_K^*}^+ + \frac{d\sigma}{d\Omega_K^*}^-} = \frac{\sqrt{2\epsilon(1-\epsilon)}\sigma_{LT'}\sin\phi}{\sigma_0}$

for $Q^2 \rightarrow 0$ and unpolarized electrons relation to **real photoproduction** cross section

Effective Lagrangian models for strangeness production

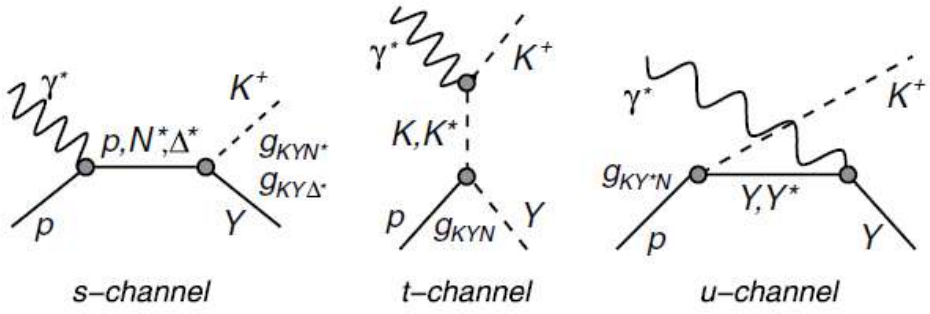

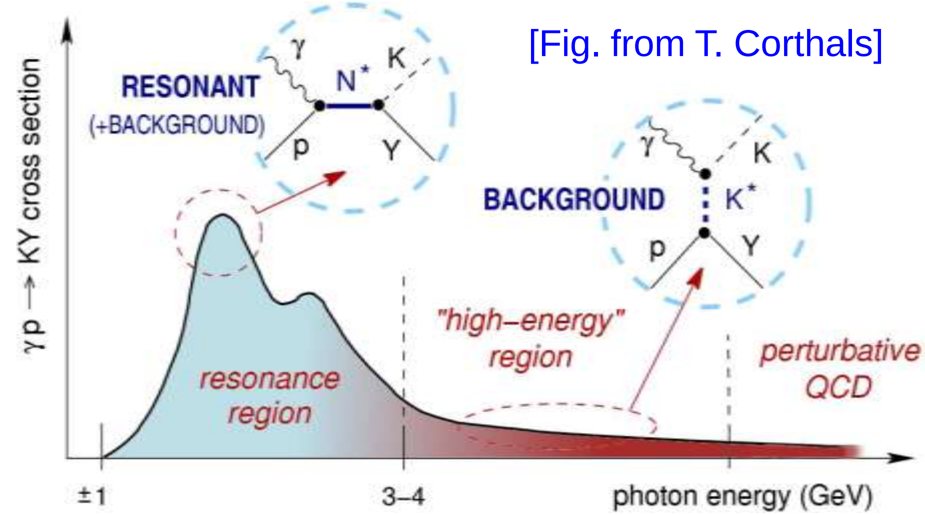

- *Saclay-Lyon A*: no hadronic f. f., SU(3), crossing symmetry,
  nucleon (spin 1/2 and 3/2) and hyperon resonances
  extended Born terms (p, Λ, Σ, K), K*(890), K_1(1270)
  [T. Mizutani *et al*., *Phys. Rev. C* 58 (1998) 75]
- *Kaon-MAID*: hadronic f. f., SU(3), no hyperon resonances,
  only nucleon (spin 1/2 and 3/2) resonances
  extended Born terms (p, Λ, Σ, K), K*(890), K_1(1270)
  [T. Mart, C. Bennhold, *Phys. Rev.* C 61 (2000) 012201(R)]
- *RPR*: Regge model for t-channel
  moderate no. of s-channel nucleon resonances
  [T. Corthals, D.G. Ireland, T. Van Cauteren, J. Ryckebusch, *Phys. Rev. C* 75, (2007) 045204]

Comparison of electro- with photoproduction

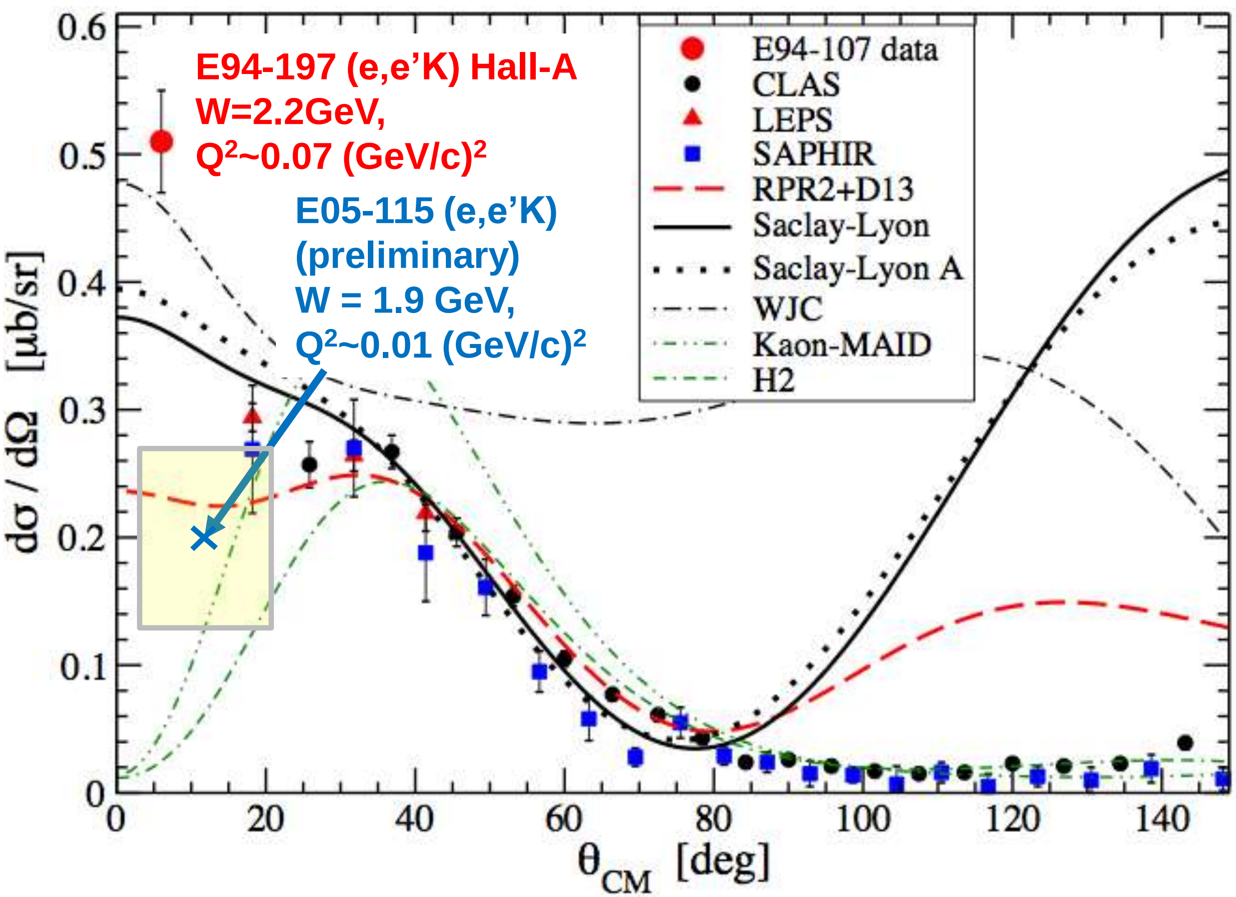

Measurements at MAMI can confirm or exclude strong Q^2 dependence

Predictions for MAMI kinematics

dσ/dΩ schematically as a function of Q^2 and *W*

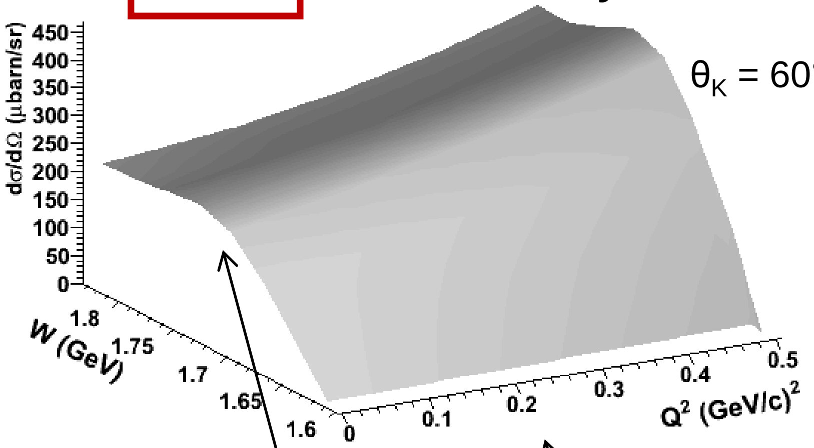

θ_K = 60° and ε = 0.5

W-dependence

Q^2-dependence

interference structures

$d\sigma_{TL'}/d\Omega$ as a function of W

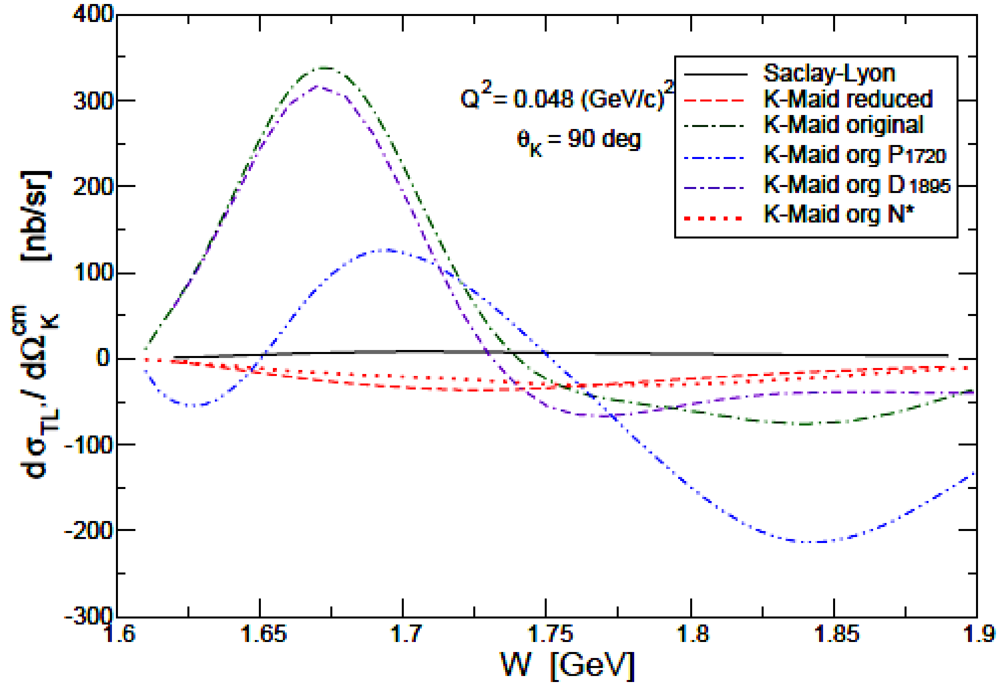

Measurements at MAMI

Electroproduction off the nucleon with MAMI-C

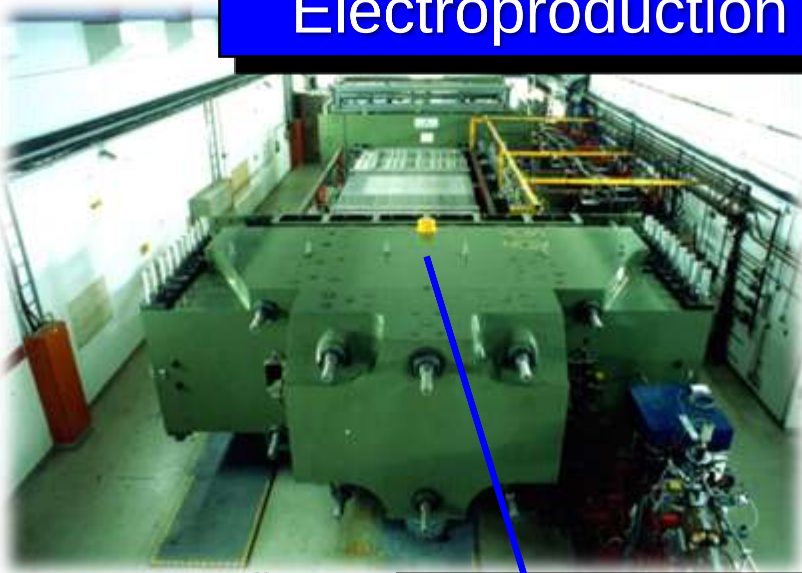

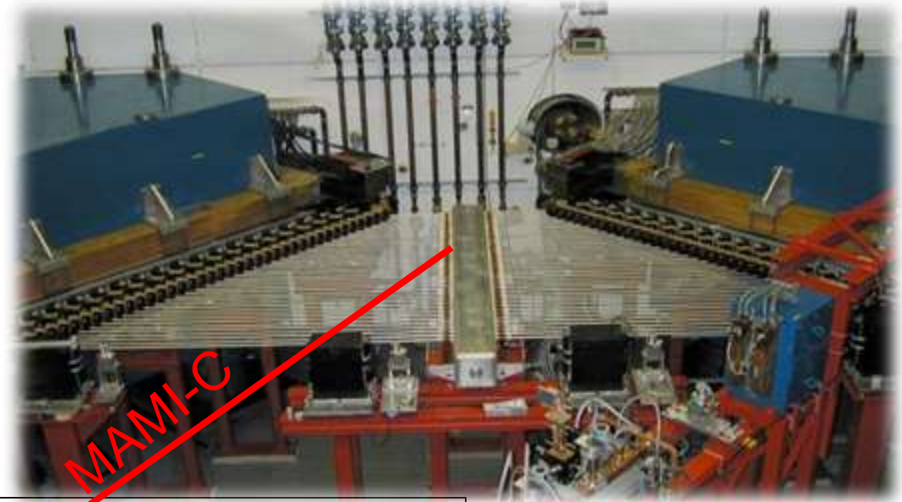

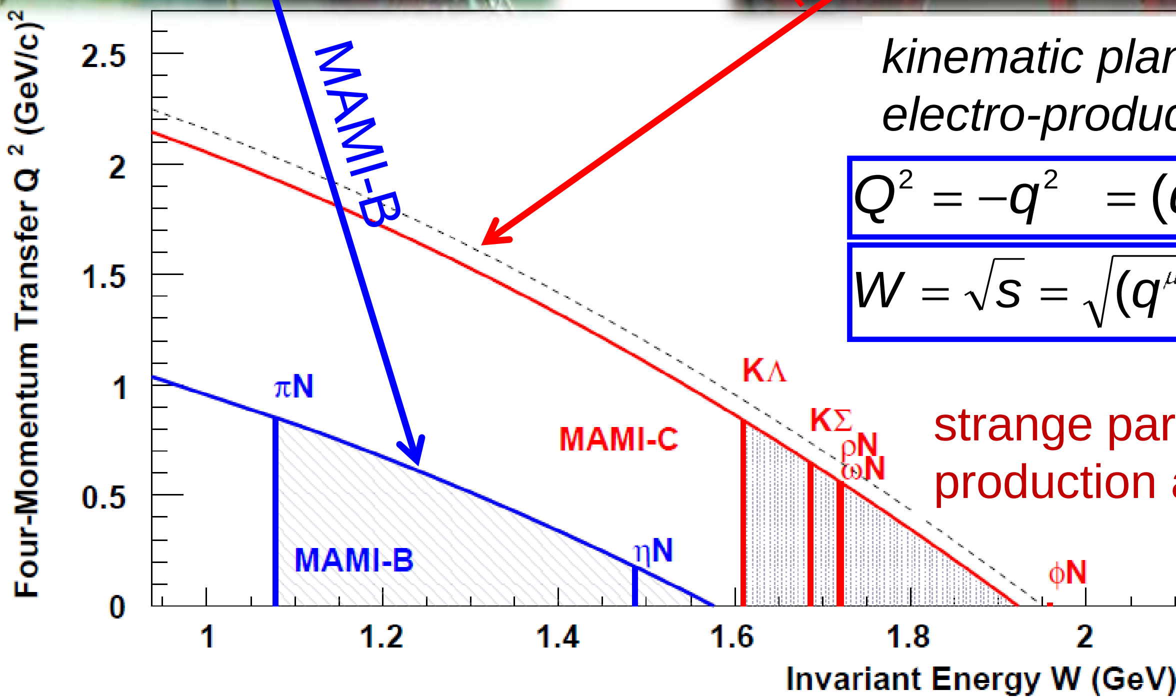

kinematic plane in electro-production:

$$Q^2 = -q^2 \quad = (q_e^\mu - q_{e'}^\mu)^2$$

$$W = \sqrt{s} = \sqrt{(q^\mu + p_{\text{target}}^\mu)^2}$$

strange particle and fragment production at W > 1.6 GeV

Magnetic spectrometer facility at MAMI

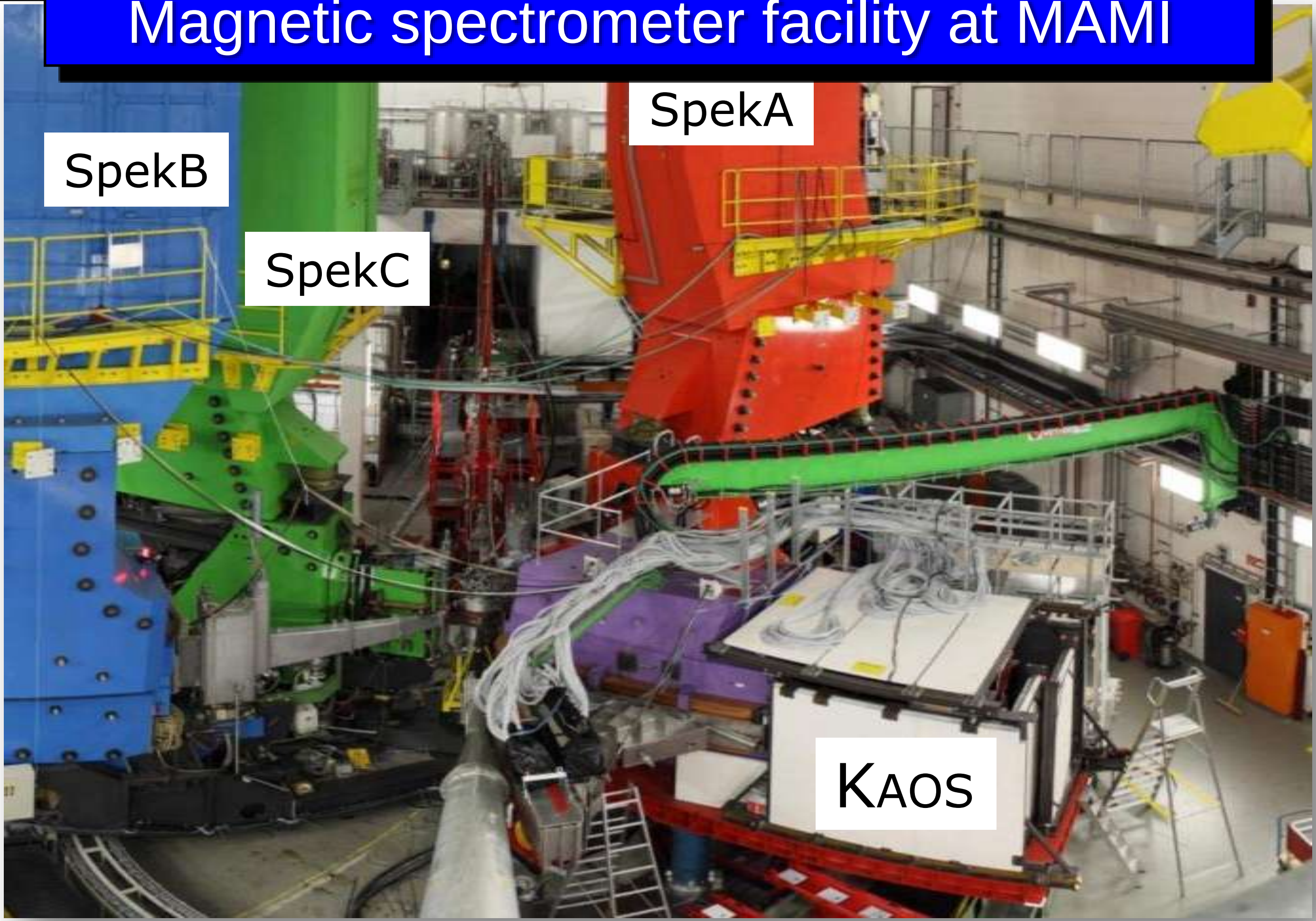

Magnetic focusing spectrometers:

- three high resolution $\Delta p/p \sim 10^{-4}$ spectrometers (SpekA,B,C)
- one short orbit spectrometer (KAOS, since 2008)

Møller polarimeter, neutron detectors, pion spectrometer …

Kaon identification

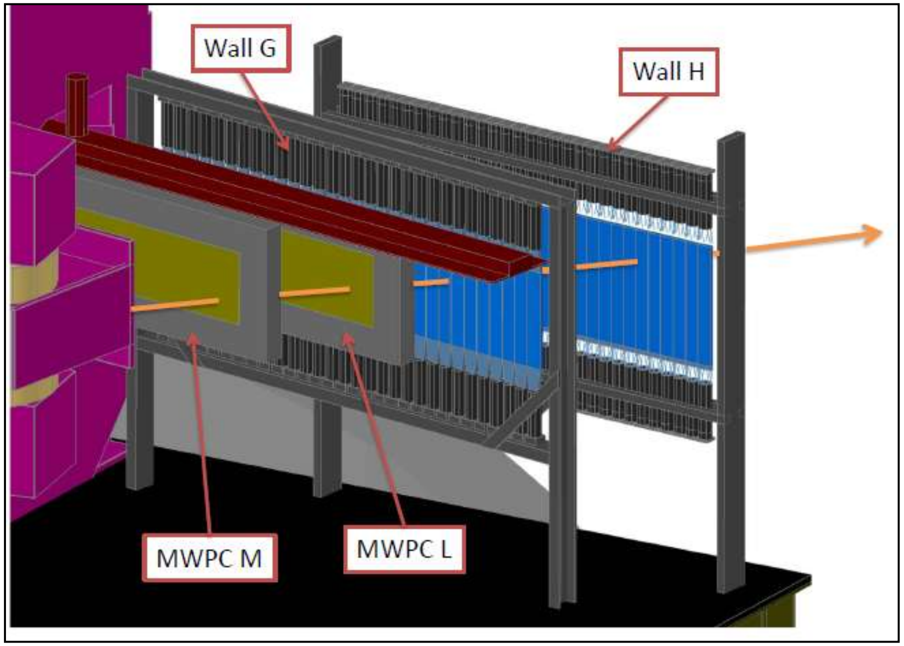

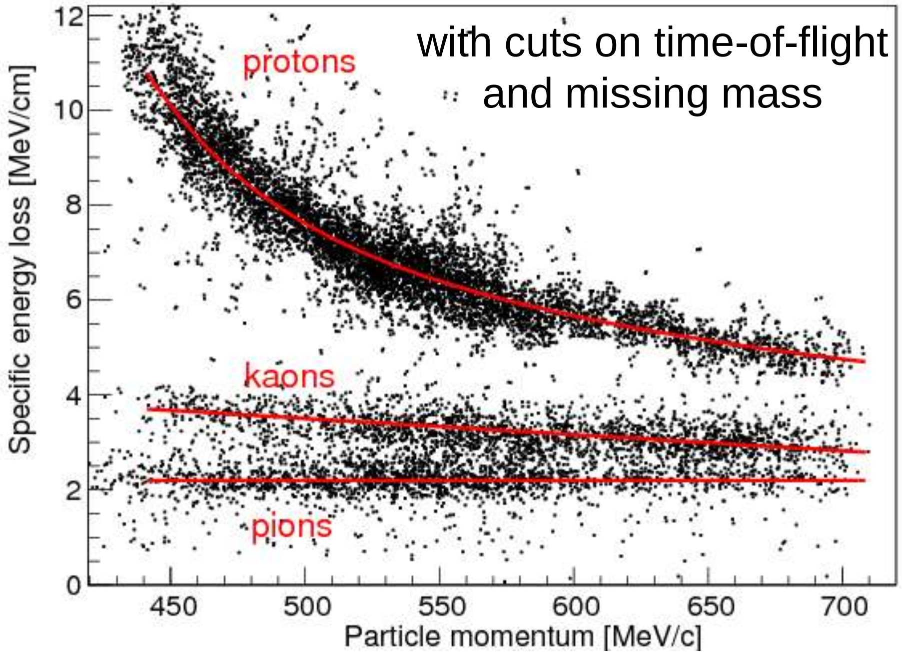

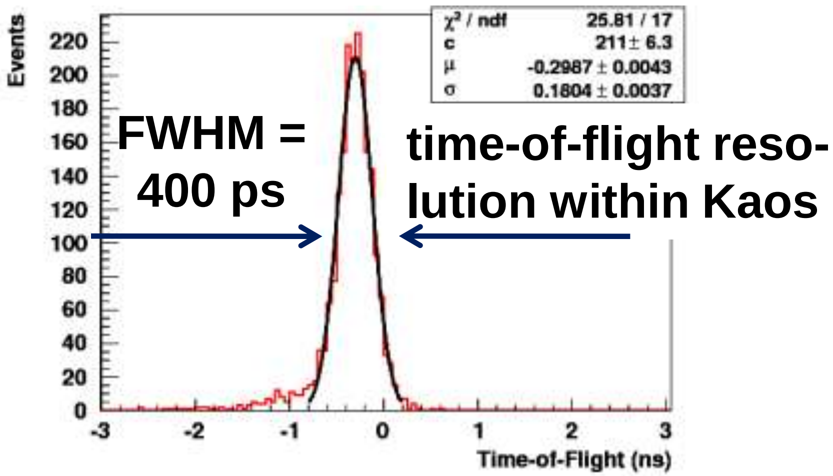

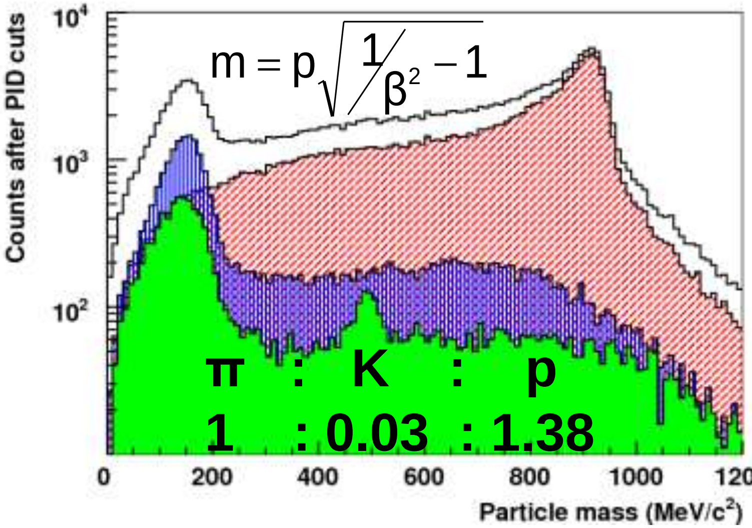

Reaction identification

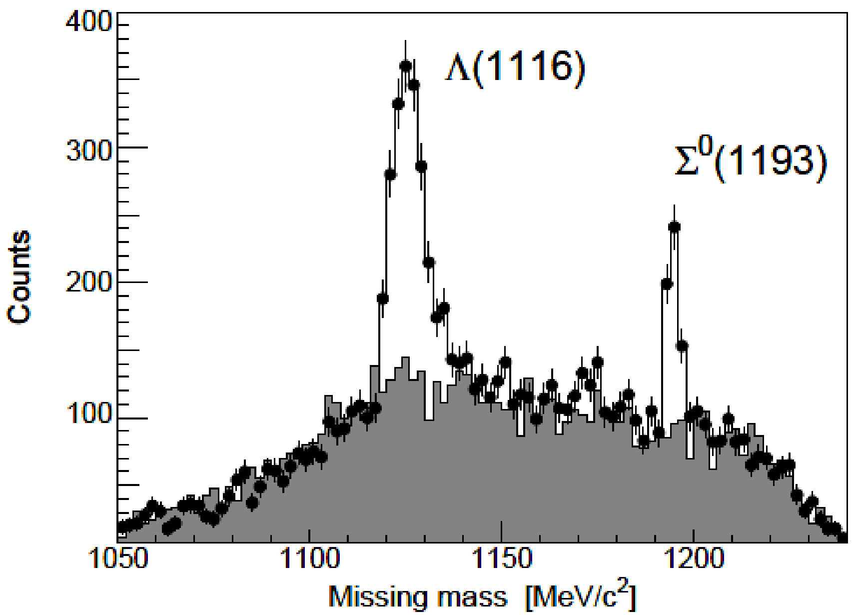

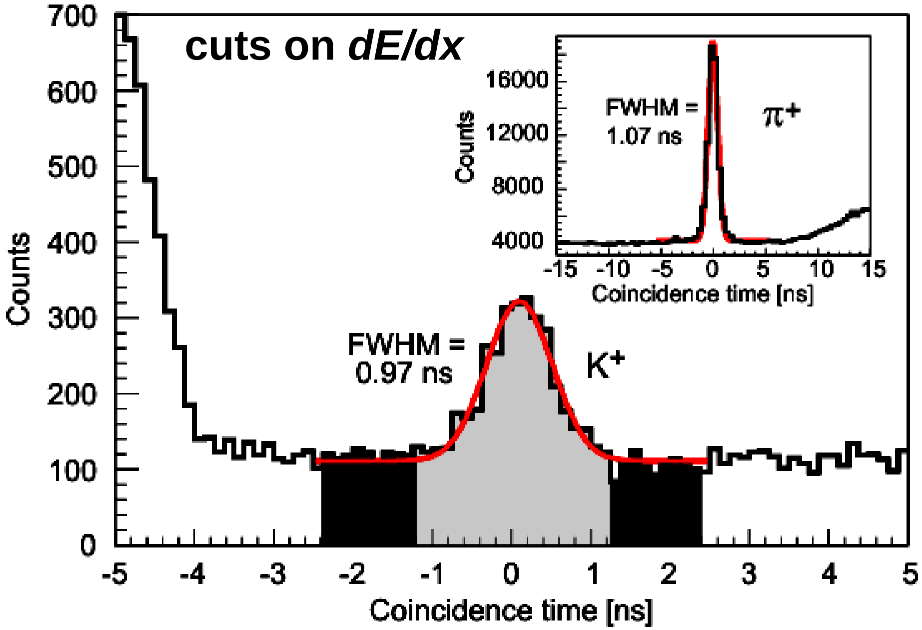

$$
\begin{aligned}
E_X &= E_e - E_{e'} + M_{targ} - E_K = \omega + M_{targ} - E_K, \\
\vec{P}_X &= \vec{q} - \vec{p}_K,
\end{aligned}
$$

extraction of cross-section using background-corrected kaon-Λ yield,

luminosity, acceptance, efficiencies, kaon survival, radiative corrections:

$$
Y = L \times \int \left[\Gamma(Q^2, W) \frac{d^2\sigma}{d\Omega_K^*} \right] A(d^5V) R(d^5V) dQ^2 dW d\phi_e d\Omega_K^*
$$

KΛ cross section at Q^2 = 0.036

$\langle Q^2 \rangle$ $(\mathrm{GeV}/c)^2$	$\langle W \rangle$ GeV	$\langle \epsilon \rangle$ (trans.)	$\langle \omega \rangle$ GeV
0.036	1.750	0.395	1.182

[P. Achenbach *et al*. (A1 Collaboration), Eur. Phys. J. A 48 2012)]

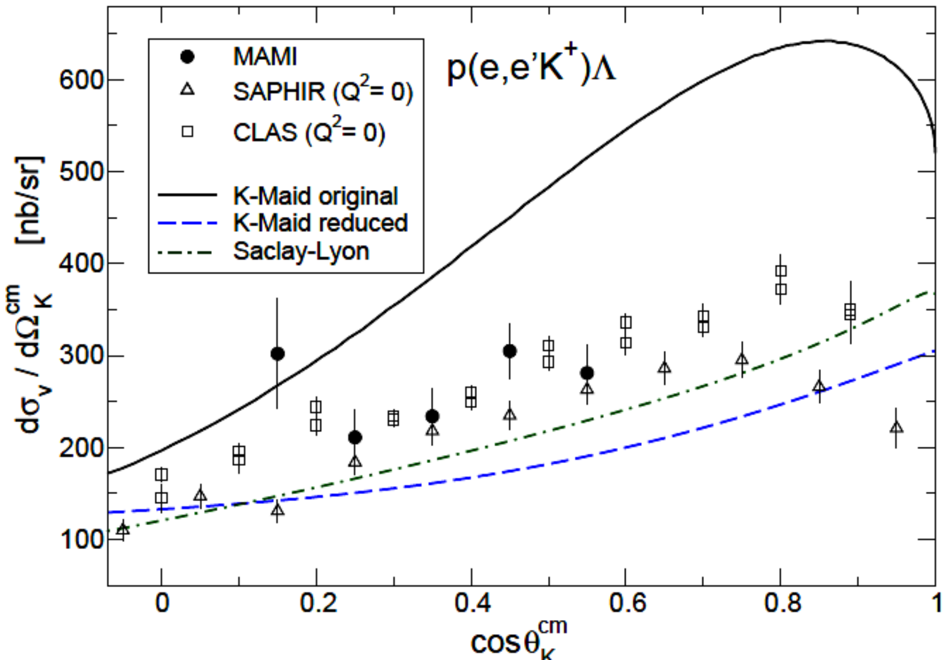

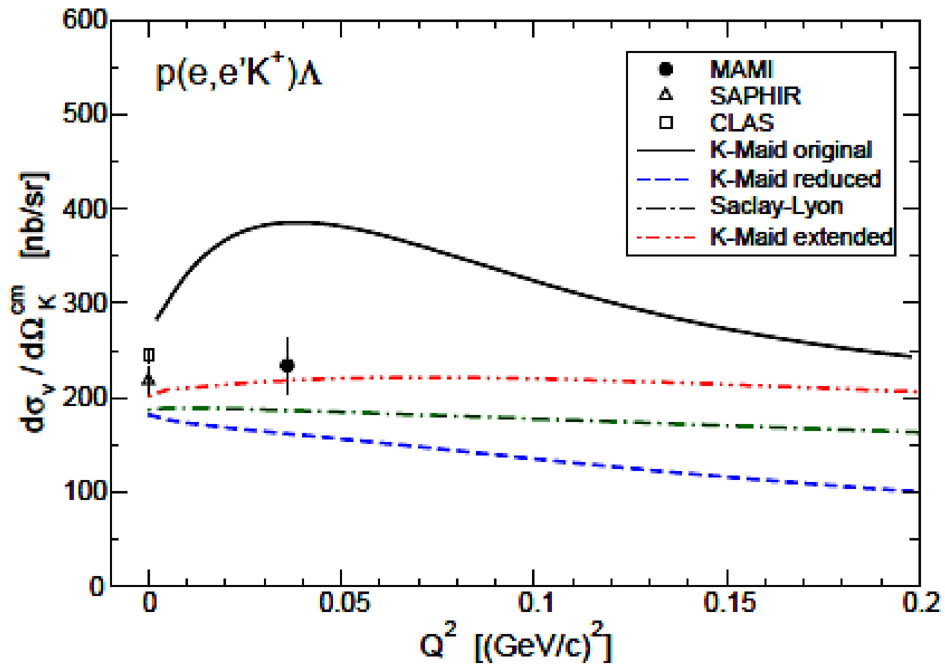

- first time measurement of cross-section at low Q^2
- only small differences to photoproduction data observed
- original Kaon-Maid model excluded with high significance

Comparison with modern isobar model variants

$\langle Q^2 \rangle$ $(\mathrm{GeV}/c)^2$	$\langle W \rangle$ GeV	$\langle \epsilon \rangle$ (trans.)	$\langle \omega \rangle$ GeV
0.036	1.750	0.395	1.182

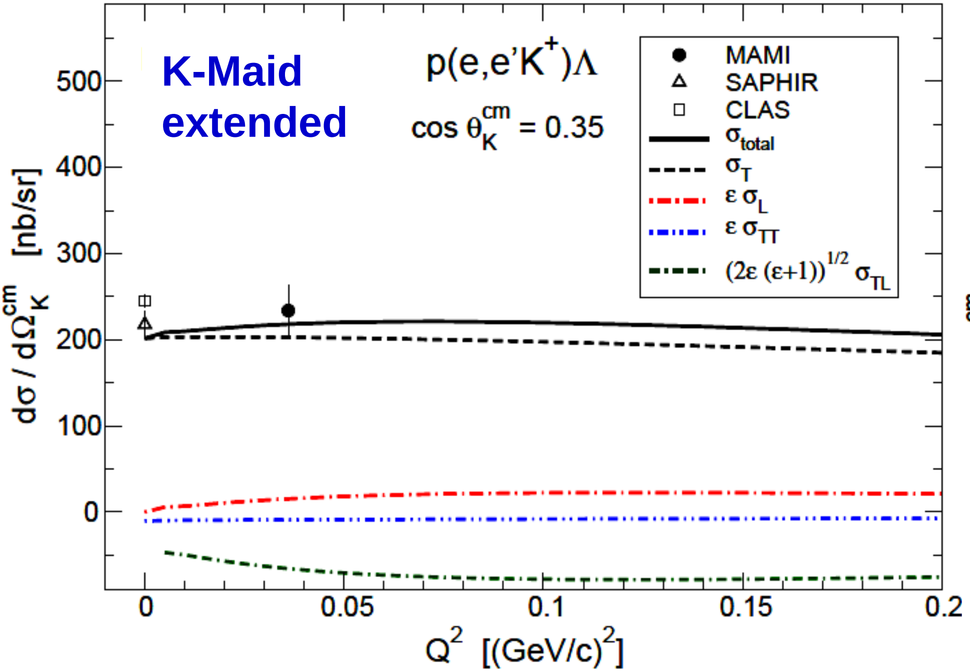

[K-Maid extended provided by T. Mart]

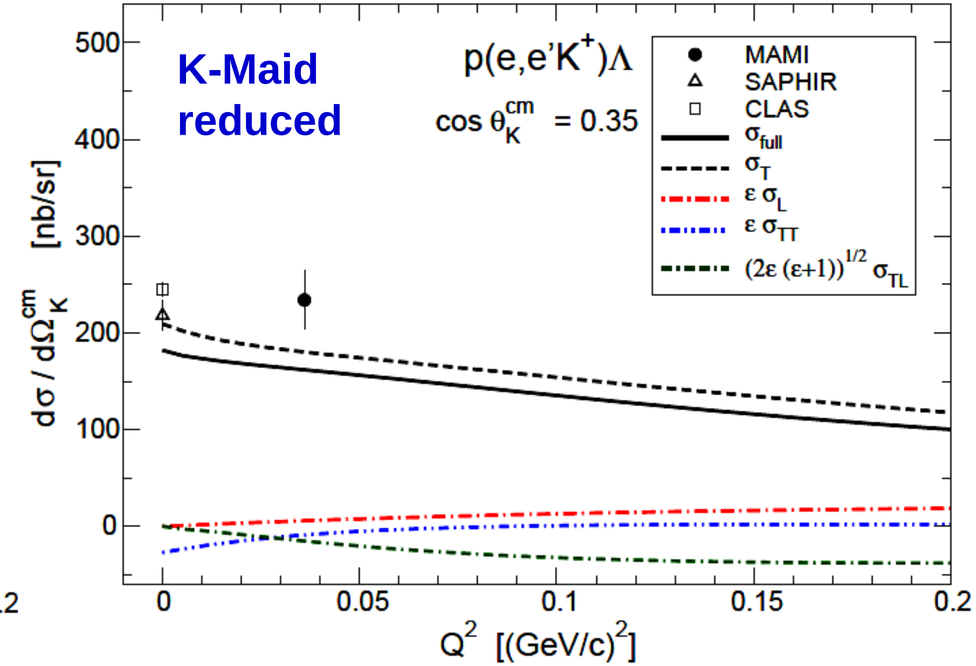

[K-Maid reduced provided by P. Bydžovský]

modern isobar models use small or vanishing longitudinal couplings

Experiments on hypernuclei and hyperfragments

Hypernuclear production methods

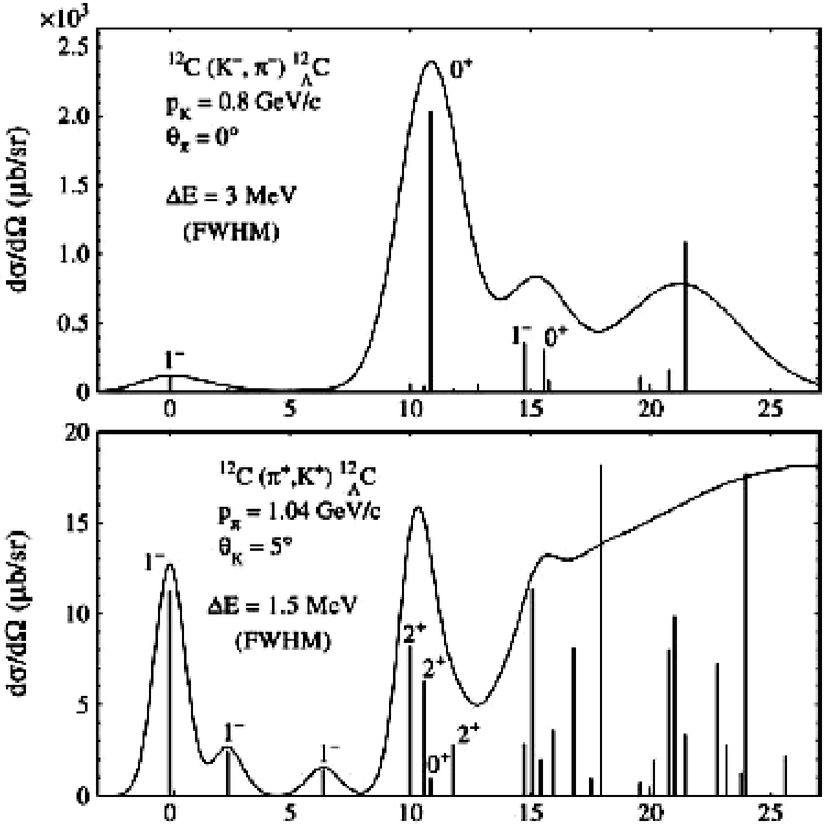

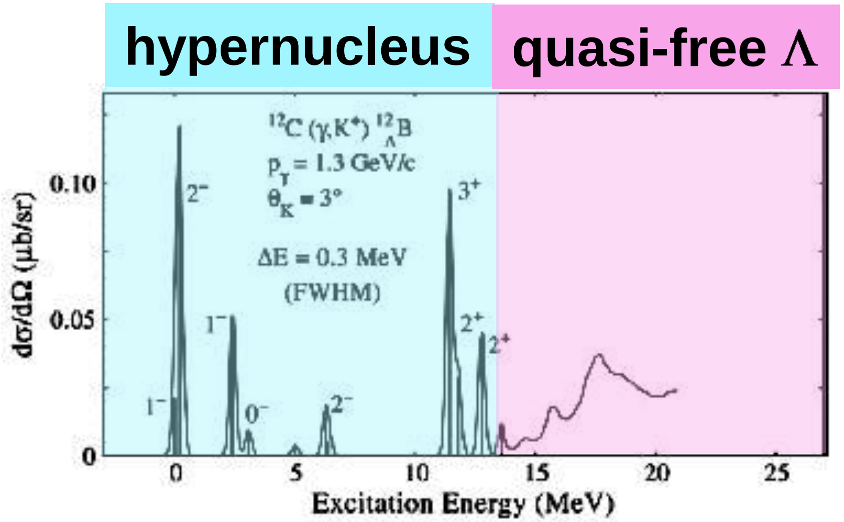

[O. Hashimoto and H. Tamura, *Prog. Part. Nucl. Phys. 57,* 564 (2006).]

two regimes for hypernuclear and hyperfragment production:

- bound hypernuclear states
- highly excited quasi-free region

First approach: missing mass spectroscopy

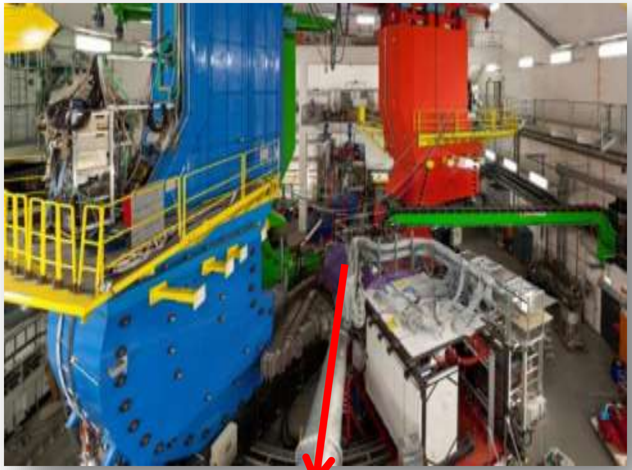

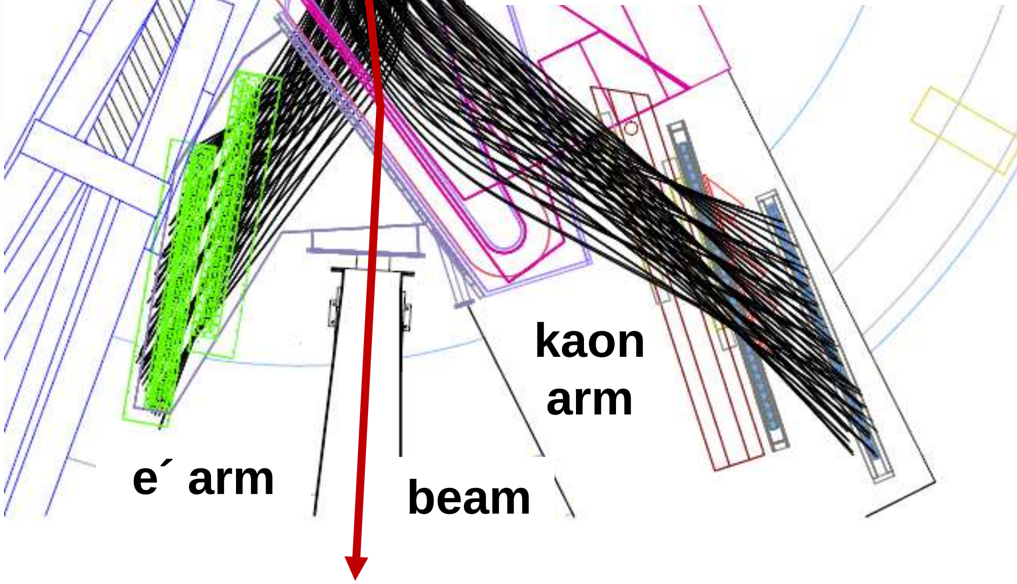

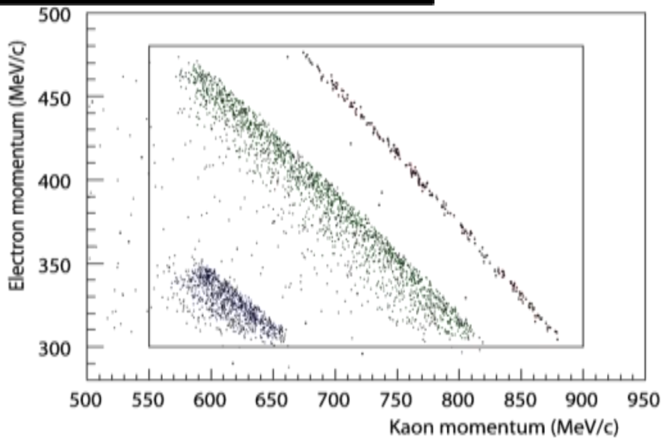

experimental requirements:

→ double spectroscopy in a single spectrometer

→ near zero-degree electron detection to maximize flux

→ low-Z targets ^{6,7}Li, ^{9}Be, ^{12}C

status: experimental setup is prepared and hypernuclear missing mass spectroscopy will be done in Mainz

Second approach: decay-pion spectroscopy

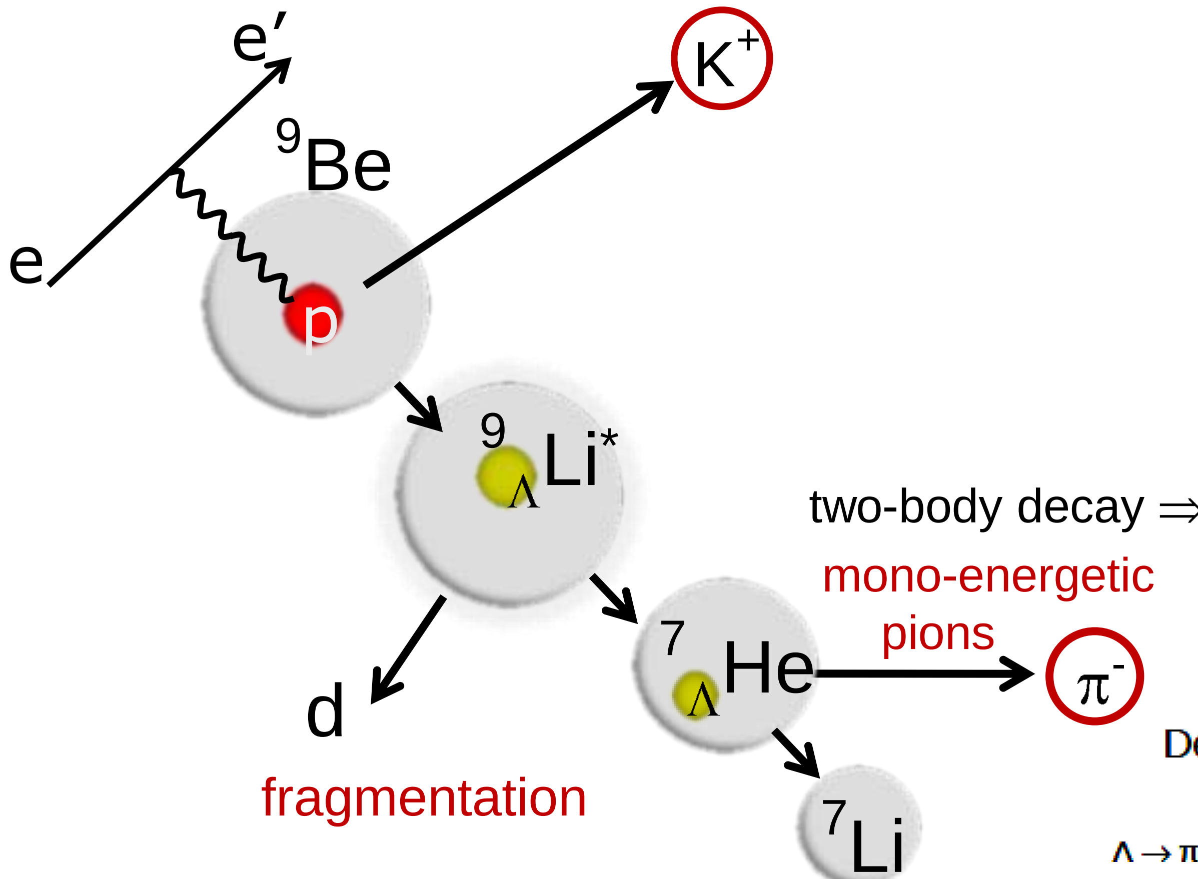

Decay of free Λ

$\Lambda \rightarrow \pi^- + p + 38$ MeV (64 %)
$\Lambda \rightarrow \pi^0 + n + 41$ MeV (36 %)

$\tau = 263$ ps

status: first experiments have been performed in Mainz with Be target

Accessible hypernuclei

decay pion sepctroscopy

PROTON NUMBER	1	2	3	4	5	6	7	8	9	10	11	12	13	14	15	16	17	18	19	20
12		^{12}C	Target				$^{20}_{\Lambda}$Mg	$^{21}_{\Lambda}$Mg	$^{22}_{\Lambda}$Mg	$^{23}_{\Lambda}$Mg	$^{24}_{\Lambda}$Mg	$^{25}_{\Lambda}$Mg	$^{26}_{\Lambda}$Mg	$^{27}_{\Lambda}$Mg	$^{28}_{\Lambda}$Mg	$^{29}_{\Lambda}$Mg	$^{30}_{\Lambda}$Mg	$^{31}_{\Lambda}$Mg	$^{32}_{\Lambda}$Mg	$^{33}_{\Lambda}$Mg
11		^{9}Be						$^{20}_{\Lambda}$Na	$^{21}_{\Lambda}$Na	$^{22}_{\Lambda}$Na	$^{23}_{\Lambda}$Na	$^{24}_{\Lambda}$Na	$^{25}_{\Lambda}$Na	$^{26}_{\Lambda}$Na	$^{27}_{\Lambda}$Na	$^{28}_{\Lambda}$Na	$^{29}_{\Lambda}$Na	$^{30}_{\Lambda}$Na	$^{31}_{\Lambda}$Na	$^{32}_{\Lambda}$Na
10		^{7}Li				$^{17}_{\Lambda}$Ne	$^{18}_{\Lambda}$Ne	$^{19}_{\Lambda}$Ne	$^{20}_{\Lambda}$Ne	$^{21}_{\Lambda}$Ne	$^{22}_{\Lambda}$Ne	$^{23}_{\Lambda}$Ne	$^{24}_{\Lambda}$Ne	$^{25}_{\Lambda}$Ne	$^{26}_{\Lambda}$Ne	$^{27}_{\Lambda}$Ne	$^{28}_{\Lambda}$Ne	$^{29}_{\Lambda}$Ne	$^{30}_{\Lambda}$Ne	$^{31}_{\Lambda}$Ne
9						$^{16}_{\Lambda}$F	$^{17}_{\Lambda}$F	$^{18}_{\Lambda}$F	$^{19}_{\Lambda}$F	$^{20}_{\Lambda}$F	$^{21}_{\Lambda}$F	$^{22}_{\Lambda}$F	$^{23}_{\Lambda}$F	$^{24}_{\Lambda}$F	$^{25}_{\Lambda}$F	$^{26}_{\Lambda}$F	$^{27}_{\Lambda}$F	$^{28}_{\Lambda}$F	$^{29}_{\Lambda}$F	$^{30}_{\Lambda}$F
8				$^{13}_{\Lambda}$O	$^{14}_{\Lambda}$O	$^{15}_{\Lambda}$O	$^{16}_{\Lambda}$O	$^{17}_{\Lambda}$O	$^{18}_{\Lambda}$O	$^{19}_{\Lambda}$O	$^{20}_{\Lambda}$O	$^{21}_{\Lambda}$O	$^{22}_{\Lambda}$O	$^{23}_{\Lambda}$O	$^{24}_{\Lambda}$O	$^{25}_{\Lambda}$O	$^{26}_{\Lambda}$O	$^{27}_{\Lambda}$O		
7				$^{12}_{\Lambda}$N	$^{13}_{\Lambda}$N	$^{14}_{\Lambda}$N	$^{15}_{\Lambda}$N	$^{16}_{\Lambda}$N	$^{17}_{\Lambda}$N	$^{18}_{\Lambda}$N	$^{19}_{\Lambda}$N	$^{20}_{\Lambda}$N	$^{21}_{\Lambda}$							
6			$^{10}_{\Lambda}$C	$^{11}_{\Lambda}$C	$^{12}_{\Lambda}$C	$^{13}_{\Lambda}$C	$^{14}_{\Lambda}$C	$^{15}_{\Lambda}$C	$^{16}_{\Lambda}$C	$^{17}_{\Lambda}$C	$^{18}_{\Lambda}$C	$^{19}_{\Lambda}$C	$^{20}_{\Lambda}$C	$^{21}_{\Lambda}$C						
5			$^{9}_{\Lambda}$B	$^{10}_{\Lambda}$B	$^{11}_{\Lambda}$B	$^{12}_{\Lambda}$B	$^{13}_{\Lambda}$B	$^{14}_{\Lambda}$B	$^{15}_{\Lambda}$B	$^{16}_{\Lambda}$B	$^{17}_{\Lambda}$B	$^{18}_{\Lambda}$B								
4		$^{7}_{\Lambda}$Be	$^{8}_{\Lambda}$Be	$^{9}_{\Lambda}$Be	$^{10}_{\Lambda}$Be	$^{11}_{\Lambda}$Be	$^{12}_{\Lambda}$Be	$^{13}_{\Lambda}$Be	$^{14}_{\Lambda}$Be	$^{15}_{\Lambda}$Be										
3		$^{6}_{\Lambda}$Li	$^{7}_{\Lambda}$Li	$^{8}_{\Lambda}$Li	$^{9}_{\Lambda}$Li	$^{10}_{\Lambda}$Li	$^{11}_{\Lambda}$Li	$^{12}_{\Lambda}$Li												
2	$^{4}_{\Lambda}$He	$^{5}_{\Lambda}$He	$^{6}_{\Lambda}$He	$^{7}_{\Lambda}$He	$^{8}_{\Lambda}$He	$^{9}_{\Lambda}$He														
1	$^{3}_{\Lambda}$H	$^{4}_{\Lambda}$H	$^{5}_{\Lambda}$H	$^{6}_{\Lambda}$H	$^{7}_{\Lambda}$H	$^{8}_{\Lambda}$H														
0	ΛN																			

NEUTRON NUMBER

missing mass sepctroscopy

$n \to \Lambda:$ (K^-,π^-)

(K^-_{stop},π^-)

(π^+,K^+)

$p \to \Lambda:$ $(e,e'K^+)$

(K^-_{stop},π^0)

$pp \to n\Lambda:$ (π^-,K^+)

Hyperfragments from a ^{9}Be target

two-body decays of 12 different hypernuclei

break-up mode	*Q* value (MeV)	π^- decay	p_π (MeV/*c*)
$^9_\Lambda$Li	-	^{9}Be + π^-	121.18
p + $^8_\Lambda$He	-13.817	^{8}Li + π^-	116.40
n + $^8_\Lambda$Li	-3.756	^{8}Be + π^-	124.12
2p + $^7_\Lambda$H	-40.328 (B_Λ=6.1)	^{7}He + π^-	135.17
d + $^7_\Lambda$He	-12.568	^{7}Li + π^-	114.61
2n + $^7_\Lambda$Li	-12.218	^{7}Be + π^-	108.02
^{3}He + $^6_\Lambda$H	-29.608 (B_Λ=5.1)	^{6}He + π^-	133.47
^{3}H + $^6_\Lambda$He	-9.745	^{6}Li + π^-	108.39
3n + $^6_\Lambda$Li	-18.957	^{6}Be + π^-	100.58
α + $^5_\Lambda$H	-11.749 (B_Λ=4.1)	^{5}He + π^-	133.42
n + α + $^4_\Lambda$H	-12.005	^{4}He + π^-	132.95
^{6}He + $^3_\Lambda$H	-18.183	^{3}He + π^-	114.29

[table prepared by L. Tang]

Realisation of stopping and decay spectroscopy

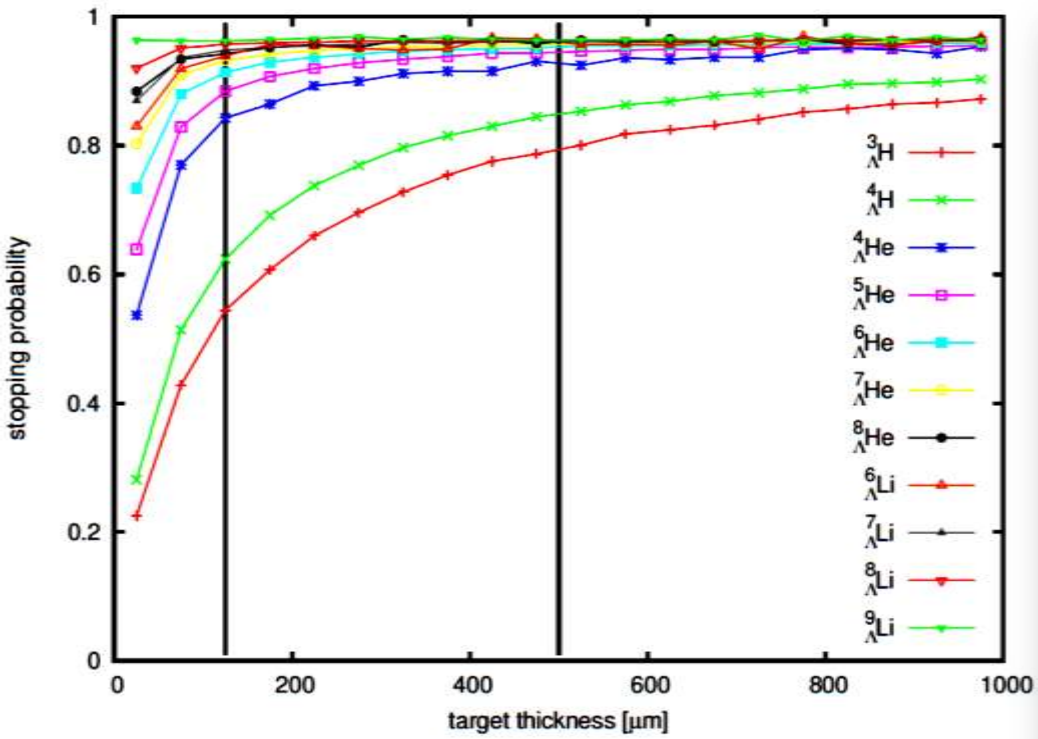

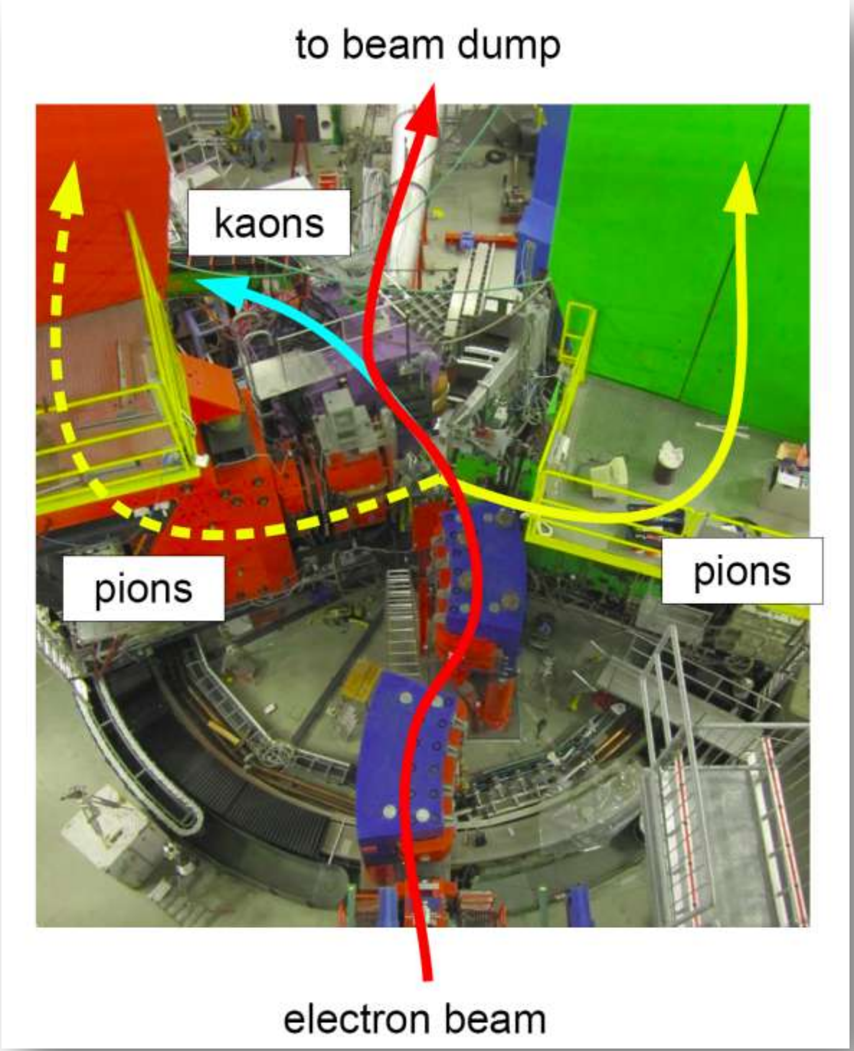

- 1500 MeV beam energy
- zero-degree kaon tagging by Kaos
- decay-pion detection with Spectrometer A & C ($\delta p/p < 10^{-4}$)

π-momentum spectrum tagged by K^+

very preliminary data
from Kaos + Spek-C (2011)

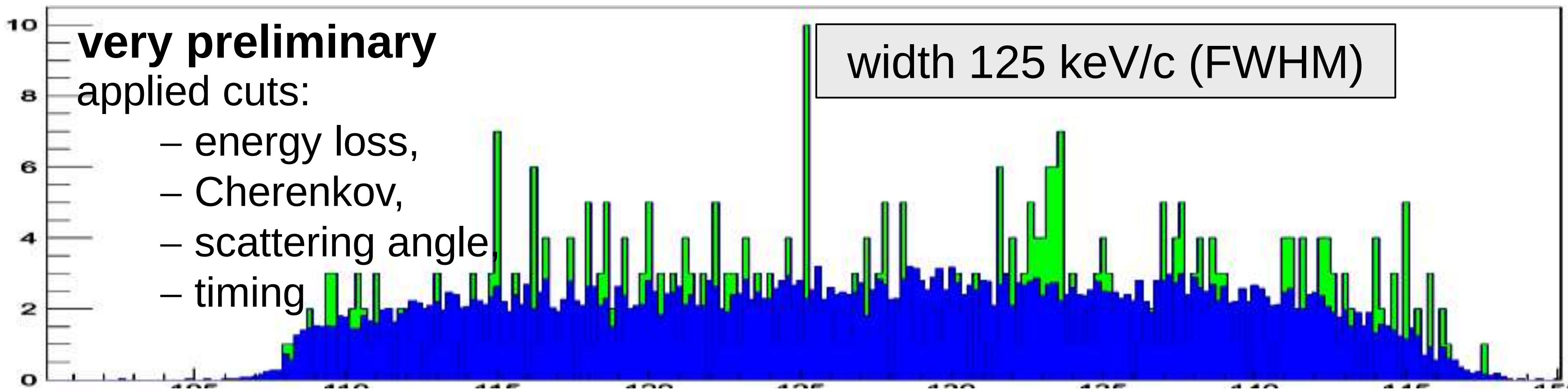

Pion momentum (MeV/c)

predicted pion spectrum for ^{9}Be target:

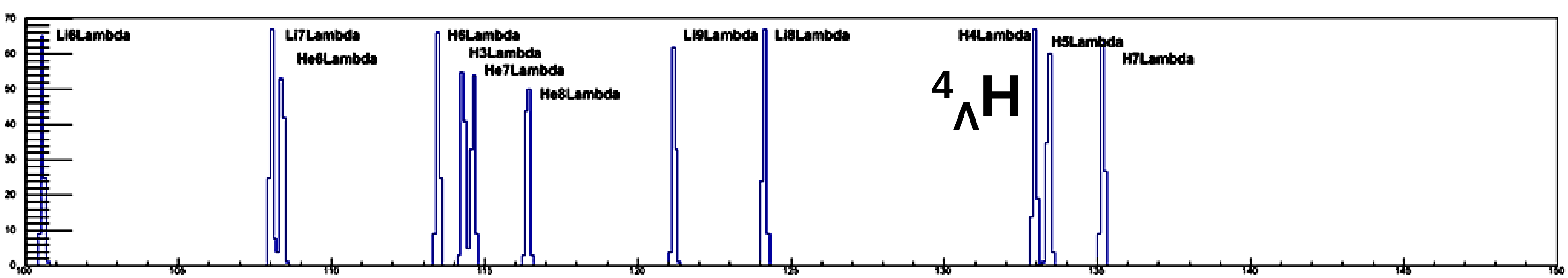

$^4_\Lambda$H and $^4_\Lambda$He emulsion data

A NEW DETERMINATION OF THE BINDING-ENERGY VALUES OF THE LIGHT HYPERNUCLEI ($A \leq 15$)

		(# of events)	B_Λ (MeV)
$^4_\Lambda$H	$\pi^- + {}^1H + {}^3H$	56	2.14 ± 0.07
	$\pi^- + {}^2H + {}^2H$	11	1.92 ± 0.12
	total	67	2.08 ± 0.06
$^4_\Lambda$He	$\pi^- + {}^1H + {}^3He$	83	2.42 ± 0.05
	$\pi^- + {}^1H + {}^1H + {}^2H$	15	2.44 ± 0.09
	total	98	2.42 ± 0.04

[M.Juric et al. Nucl. Phys B52 (1973)]

2.14 ± 0.07 → different modes

1.92 ± 0.12 → give 0.22 MeV difference

systematic error?

charge symmetry breaking effect of ΛN interaction

Double strange hypernuclear experiments

Production mechanism and detection strategy at PANDA

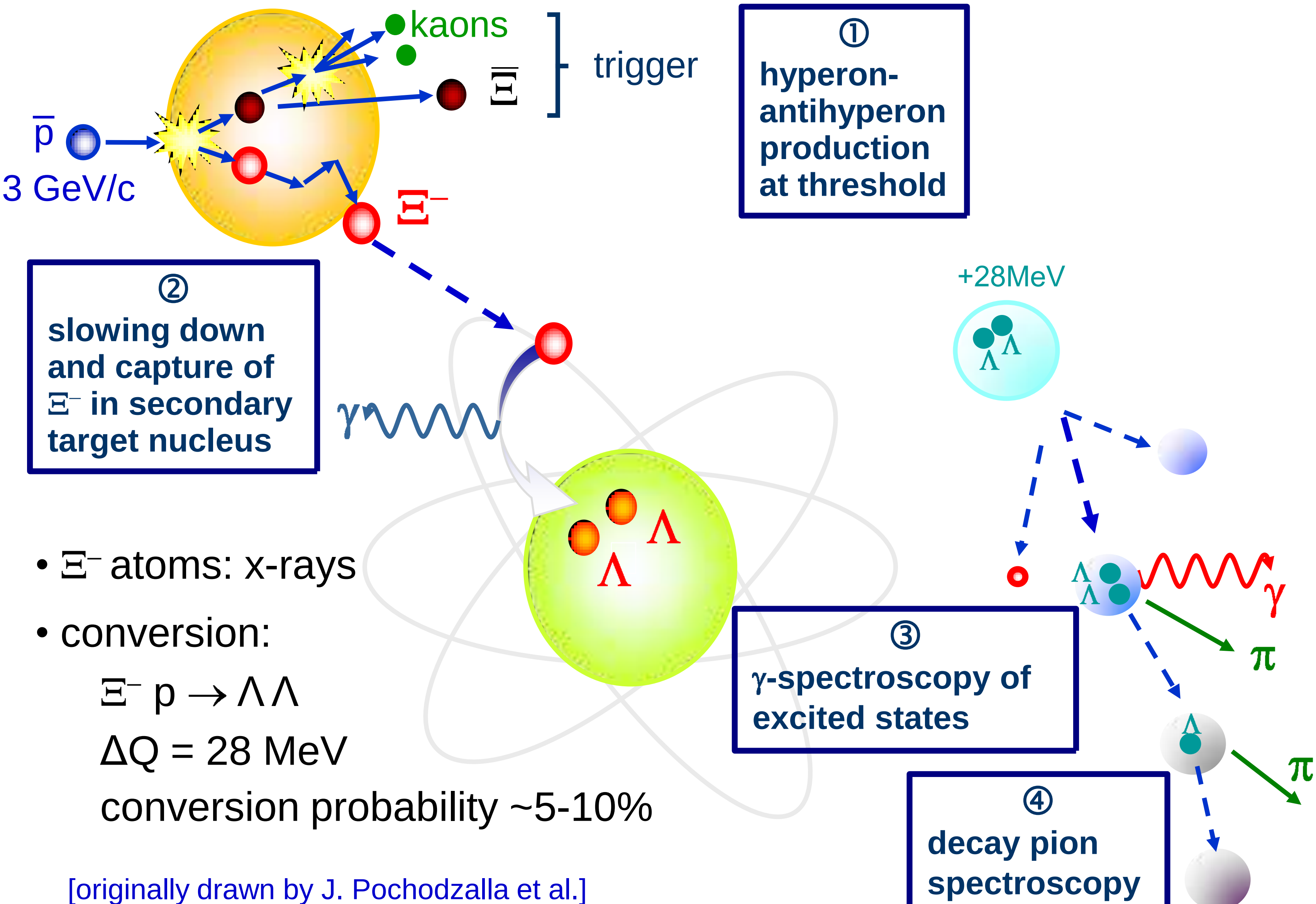

- Ξ^- atoms: x-rays
- conversion:

  $\Xi^- p \rightarrow \Lambda\Lambda$

  $\Delta Q = 28$ MeV

  conversion probability ~5-10%

[originally drawn by J. Pochodzalla et al.]

Instrumentation for hypernuclear physics at PANDA

Germanium detector array for hypernuclei spectroscopy

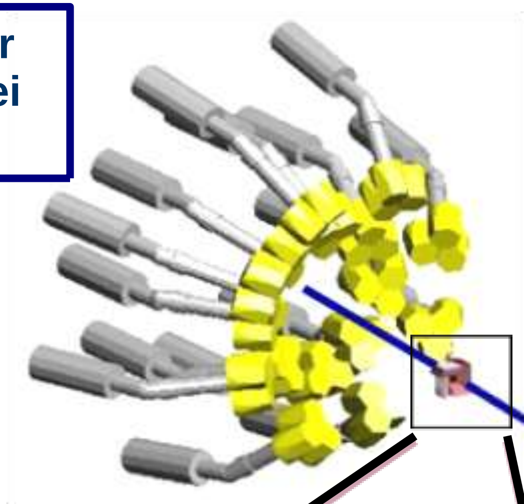

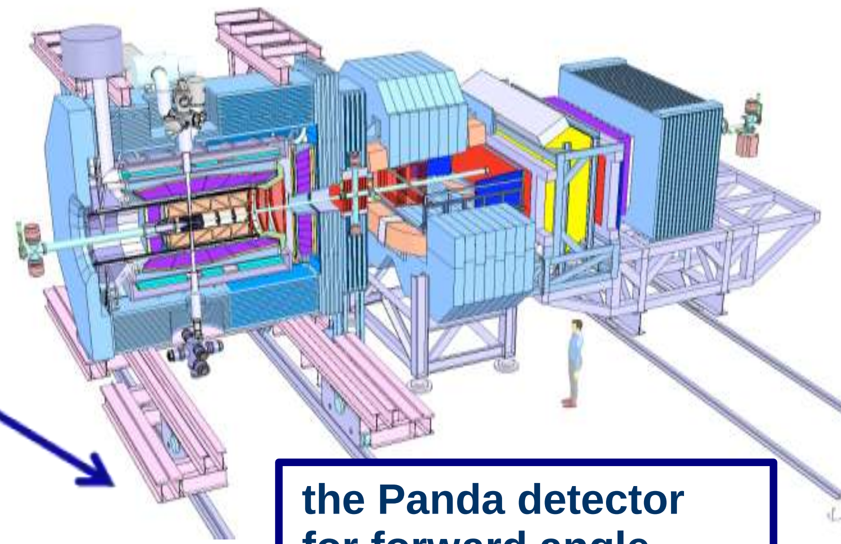

the Panda detector for forward angle particle identification

primary diamond target for Ξ production

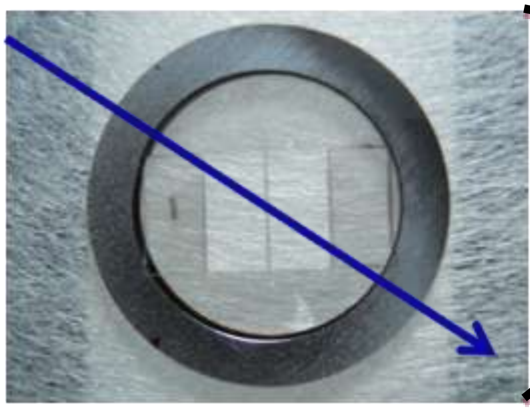

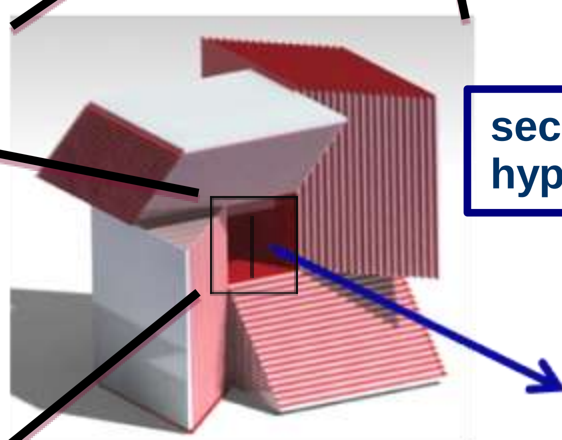

secondary target for hypernuclei formation

Prototype of thin diamond target

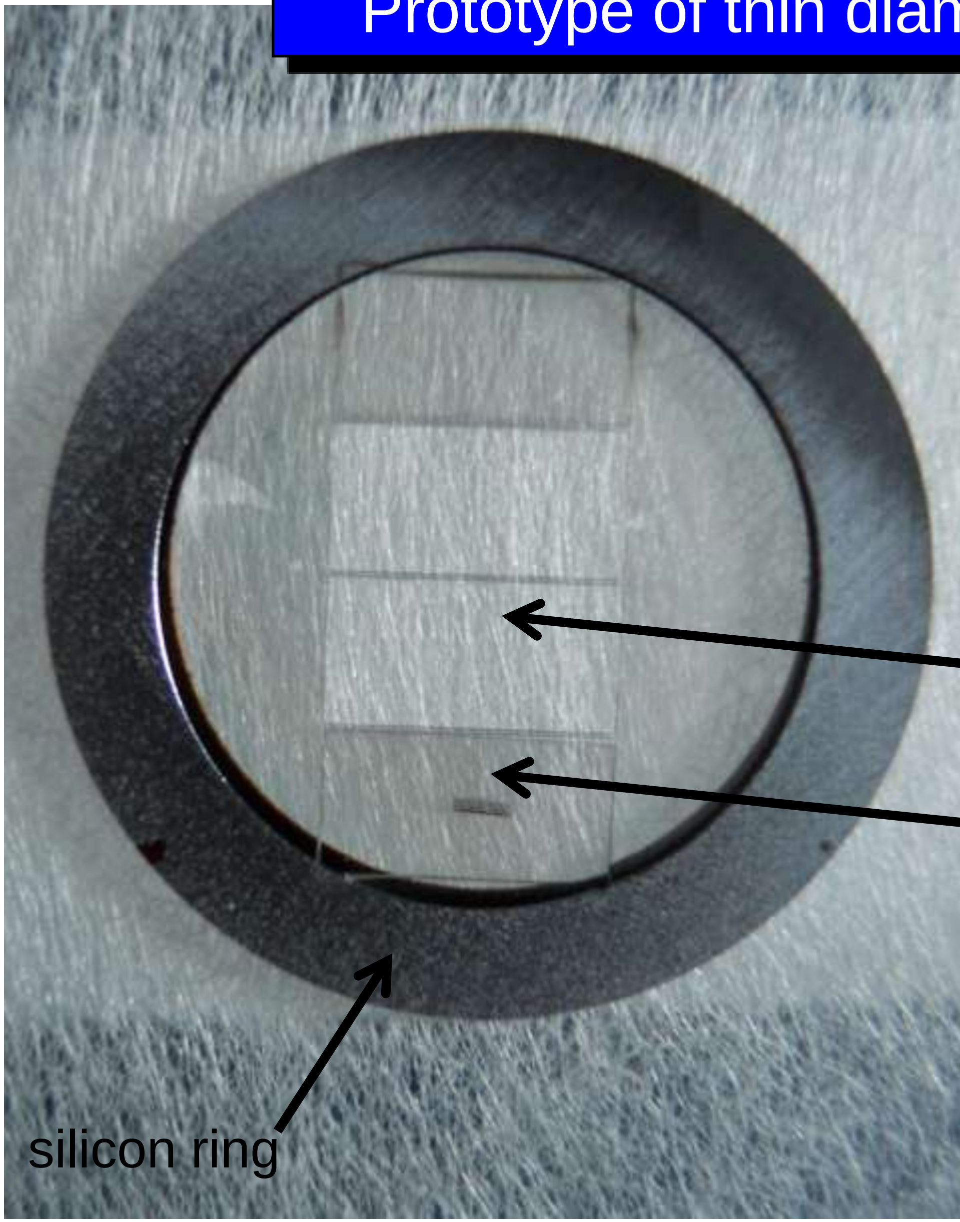

diamond wire

diamond membrane

- silicon ring inner Ø =11 mm
- diamond thickness = 3 μm
- diamond wire width = 99.9 μm

[shown by F. Iazzi, PANDA Meeting 6 Sept. 11]

Stopping of the Xi particles

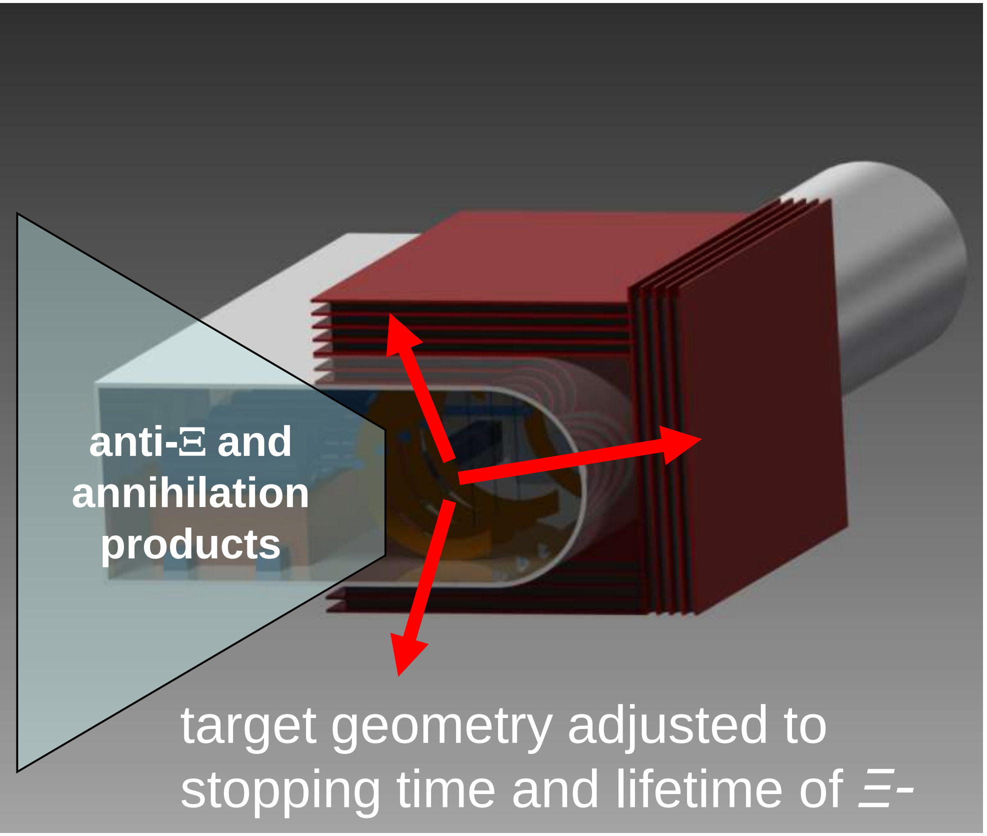

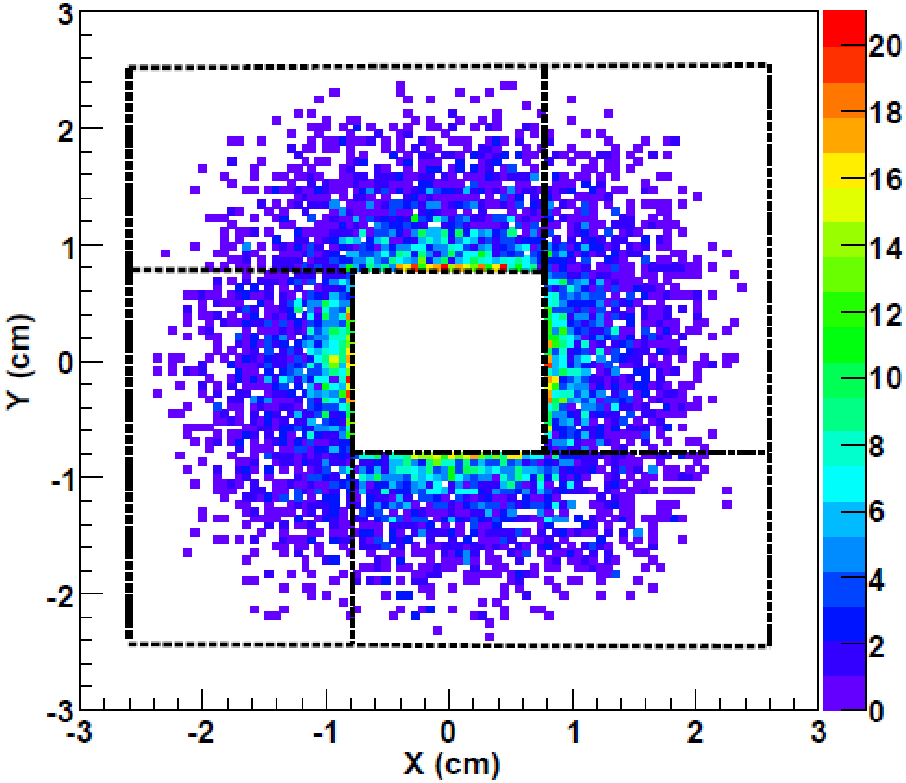

3 to 4 target blocks:
– some layers of double sided Si strip detectors
– some layers of absorbers (Be, B and C)

Prototype developments for the secondary target

frontend electronics developments:

- silicon microstrip detector tests
- optimization of target geometry

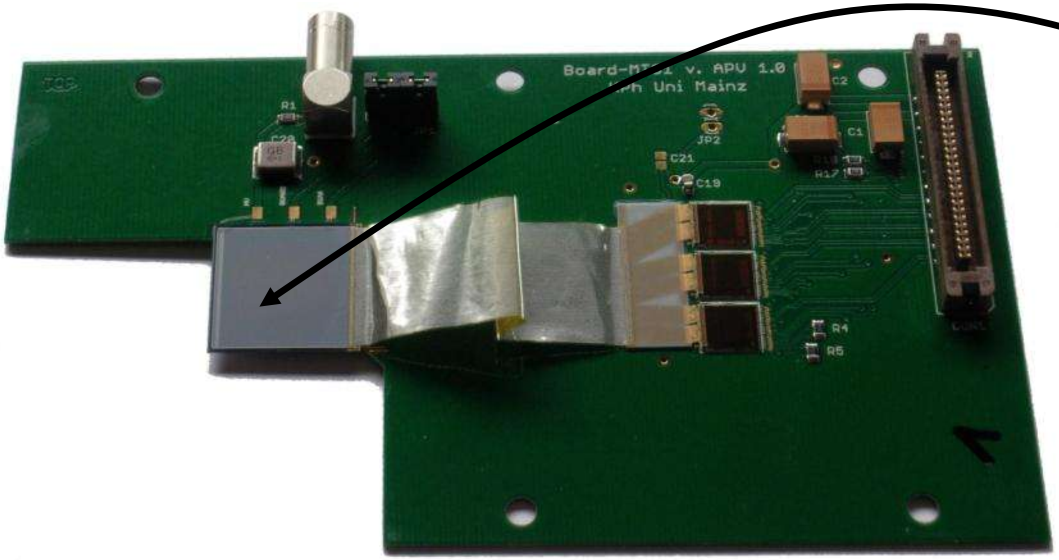

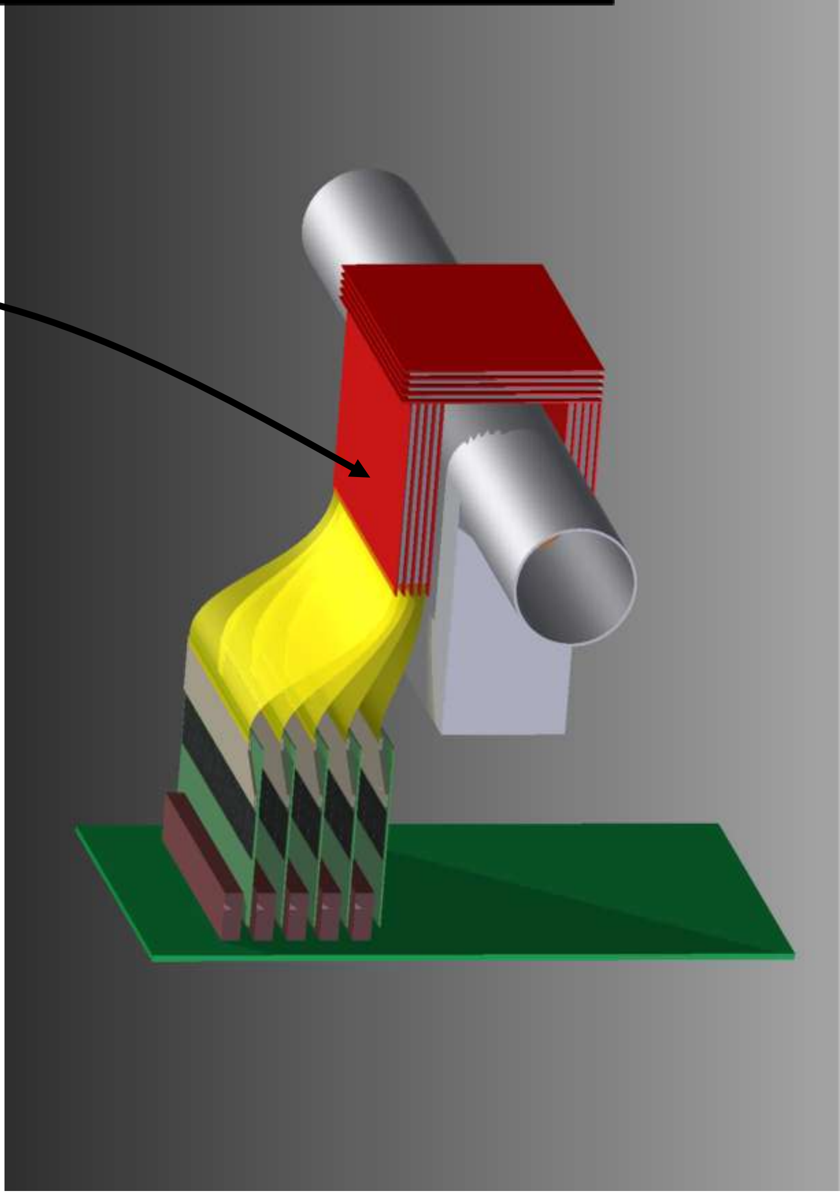

adjustment to decay pion tracking and spectroscopy

Towards a prototype of HPGe Cluster Array

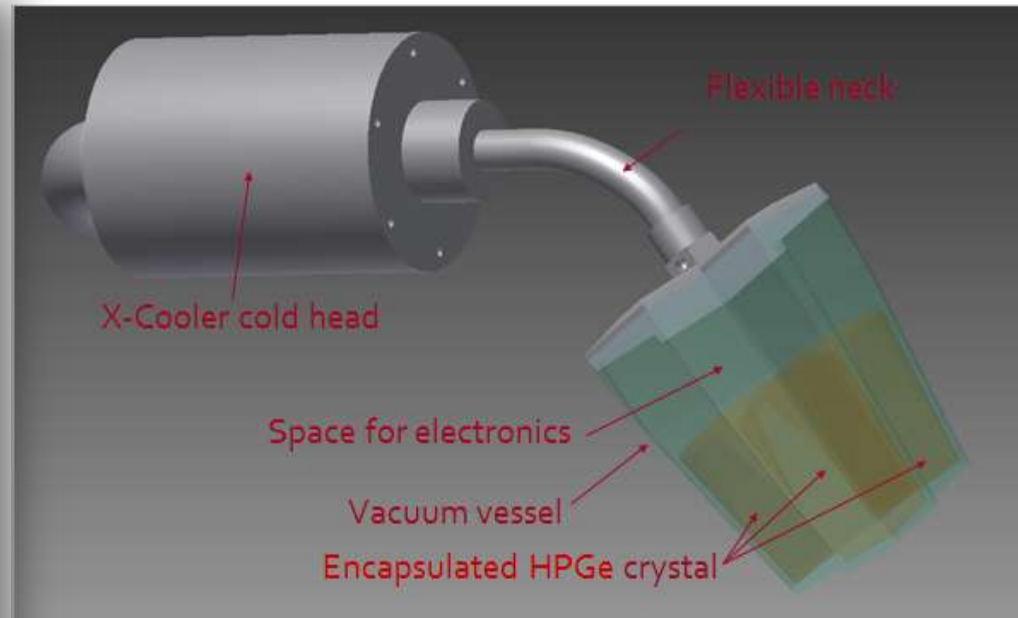

[M. Steinen, U Mainz, I. Kojouharov, GSI]

HPGe developments:

- HPGe detector tests
- electromechanical cooler performance

  FWHM = 1.83 keV @ 1332 keV

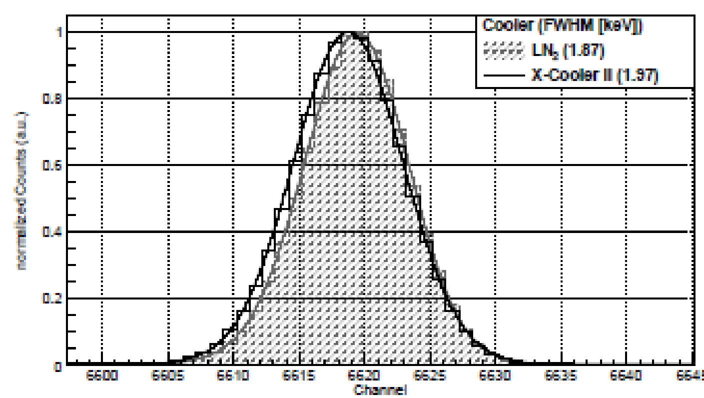

Target integration into the spectrometer

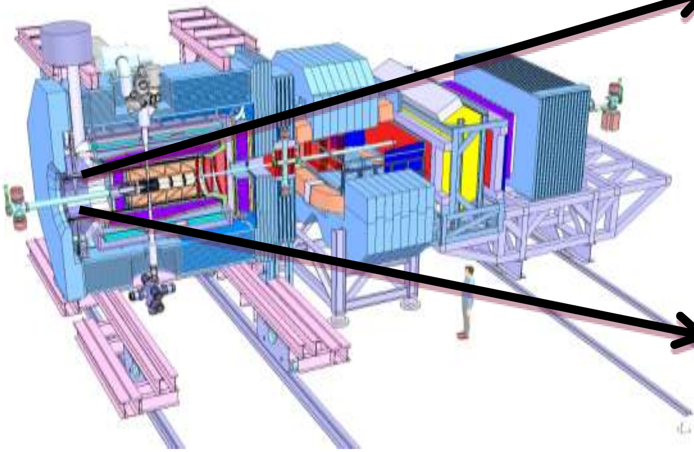

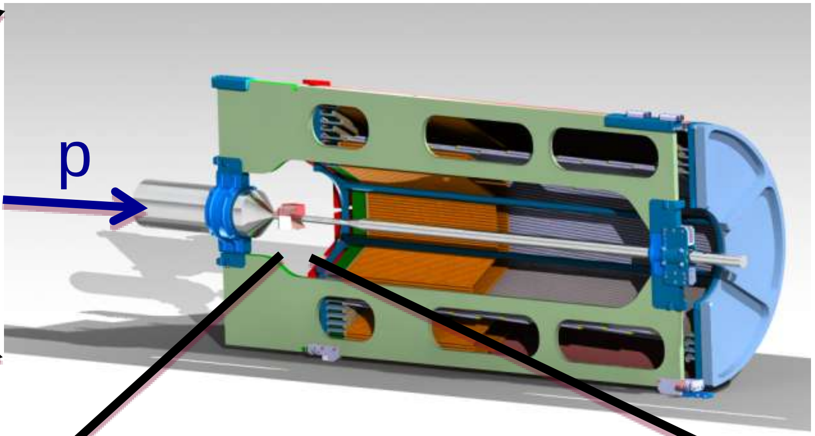

Development of structures:

- beam-pipe design
- automated primary target box
- accessibility

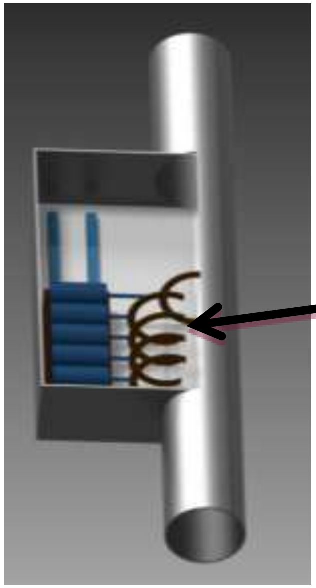

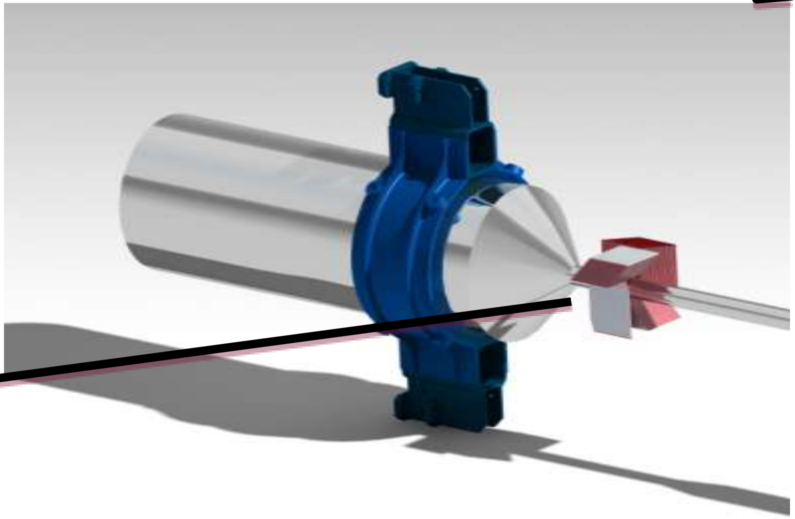

[A. Sanchez Lorente, D. Rodriguez, Shown at PANDA Meeting 6 Sept. 11]

HPGe array integration into the spectrometer

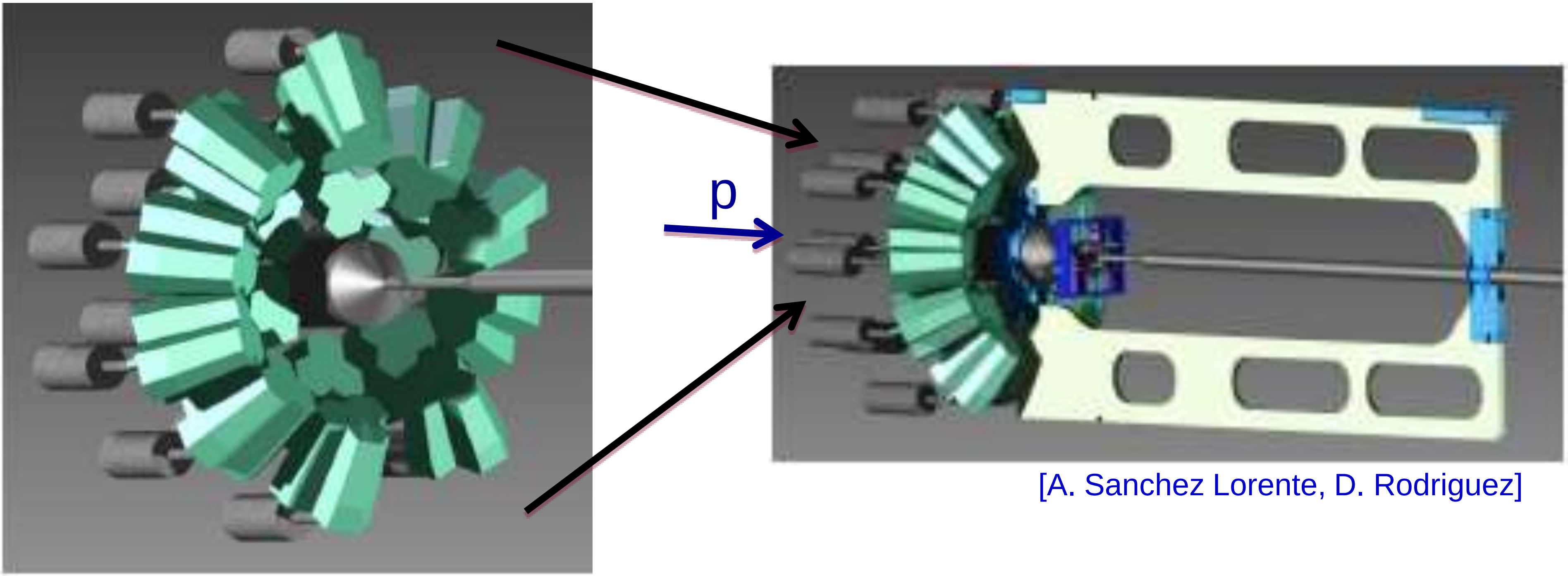

[A. Sanchez Lorente, D. Rodriguez]

Geometrical integration concept:

- $\theta_{lab} < 45°$: Ξ-bar, K trigger and PID in PANDA spectrometer
- $\theta_{lab} = 45°$-$90°$: Ξ-capture and hypernuclei formation
- $\theta_{lab} > 90°$: γ-detection with HPGe at backward angles

Background suppression by decay pion correlation

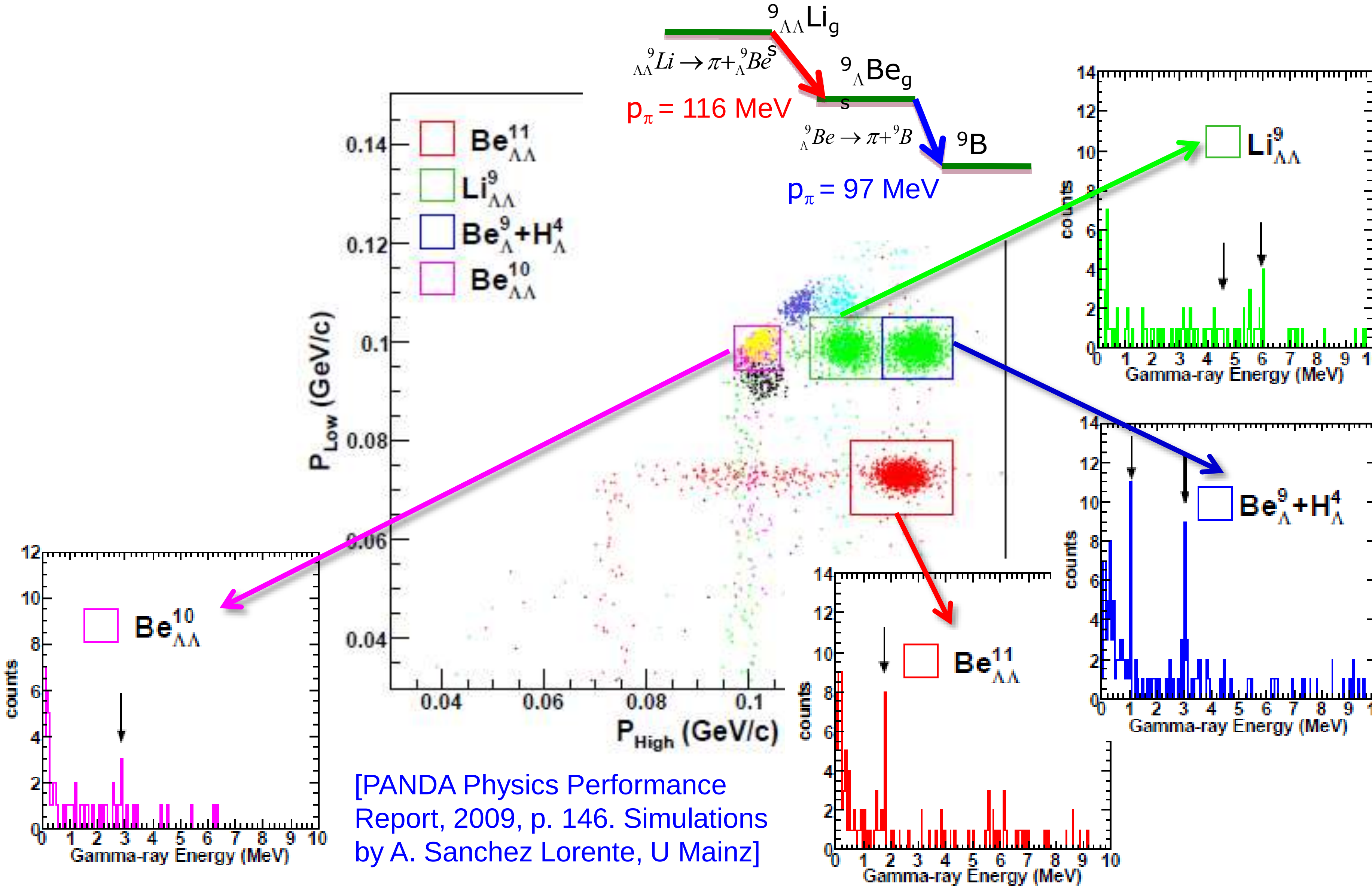

[PANDA Physics Performance Report, 2009, p. 146. Simulations by A. Sanchez Lorente, U Mainz]

Spectroscopy of ΛΛ-hypernuclei

[E. Hiyama, M. Kamimura, T.Motoba, T. Yamada and Y. Yamamoto, Phys. Rev. 66 (2002), 024007]

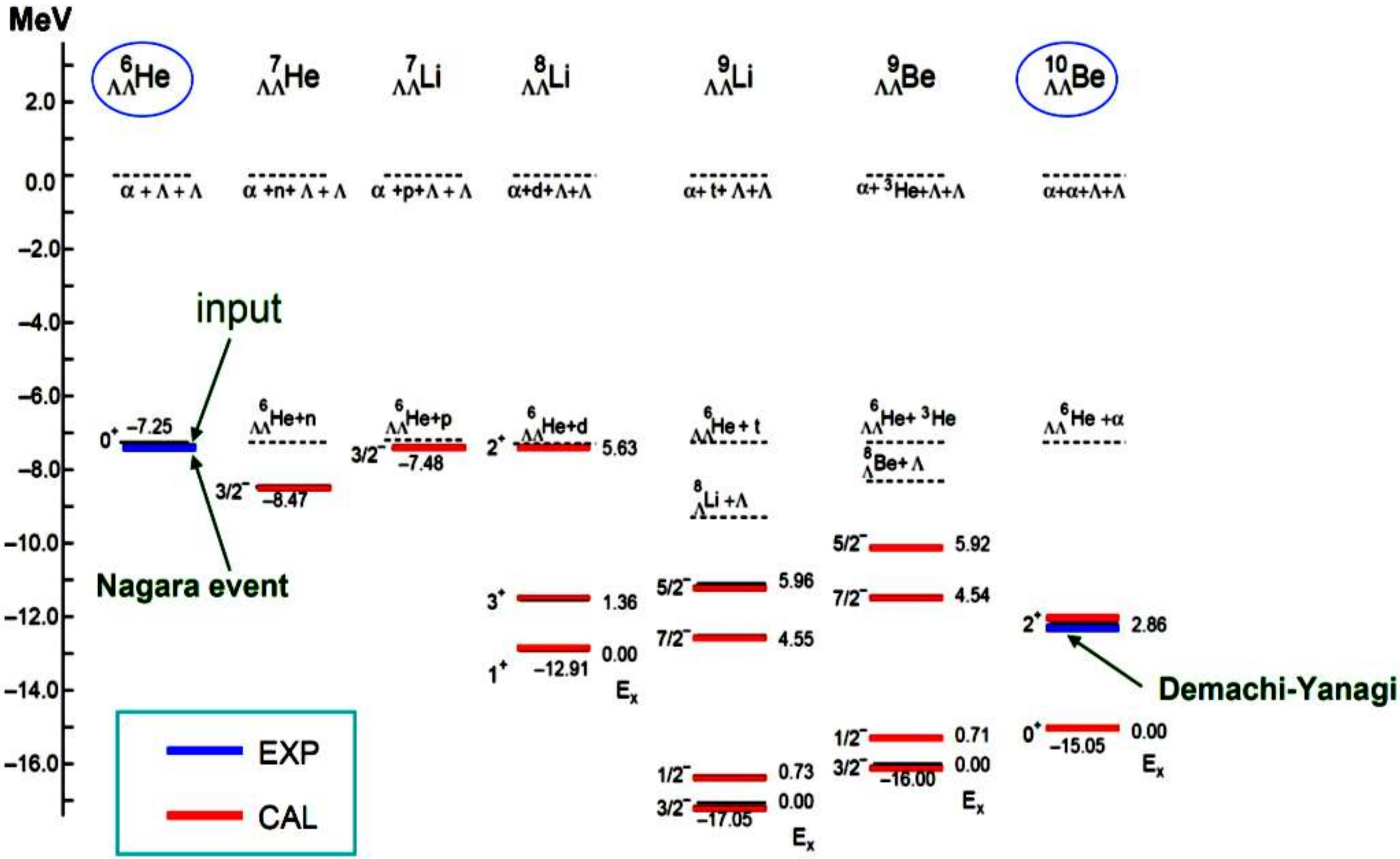

- many excited, particle stable states in double hypernuclei predicted
- level structure reflects levels of core nucleus

Summary

- Hypersystems provide a link between nuclear physics and QCD to study basic properties of strongly interacting systems
- many experimental challenges to realize hypernuclear physics
- current experiments in Germany on hypernuclear physics:

peripheral heavy ion collisions at GSI

charged particle spectroscopy of single hypernuclei at MAMI

γ-spectroscopy of double hypernuclei at PANDA